Dear Editor and Reviewers:

We appreciate all of you for the thoughtful comments and suggestions, which are very helpful in improving the manuscript. We have carefully considered all the comments and revised the manuscript accordingly. The major revisions are summarized as follows.

First, we expanded the sensitivity experiments. We conducted additional experiments to investigate the sensitivity of TOA scalar and polarized reflectance to aerosol parameters, including the phase matrix. In addition, we provided the error bounds to better quantify the associated errors.

Second, we improved and clarified the methodological description. We refined the presentation of the retrieval algorithm by explicitly describing the compositions of the measurement vector, state vector, and a priori information. We clarified the observational channels, viewing geometries, and polarization characteristics used in the algorithm, and provided further explanation of the retrieval parameters, as well as the selection of a priori constraints and their uncertainties.

Third, we strengthened the comparison with other satellite data products. In the regional and global analyses, we added more comprehensive discussions comparing our results with other satellite data sources such as MODIS, thereby improving the interpretation and validation of our findings.

Fourth, we added four summary tables to enhance readability and organization. These tables summarize the datasets used in this study, the structure of the measurement vector, the composition of the state vector, and the parameter configurations adopted in the sensitivity experiments.

In addition, we corrected bugs in the data processing workflow, updated several figures, and conducted an overall careful revision of the manuscript to improve consistency, clarity, and presentation. Detailed changes are reflected in the revised manuscript, and a point-by-point response to all comments is presented below.

Sincerely,

28 Jing Li,

29 Department of Atmospheric and Oceanic Sciences,

30 Peking University

31 jing-li@pku.edu.cn

32

Report 1

Reply to Anonymous Referee #3

The manuscript addresses an important topic in multi-angle polarimetric aerosol retrieval and makes use of valuable DPC observations. However, in its current form, the study exhibits substantial shortcomings in the justification of novelty, the description and reproducibility of the retrieval methodology, and the physical interpretation of several key results. In particular, the uncertainty characterization and its consistency with the assumed measurement accuracy are insufficiently addressed, and some systematic features in the retrieval products remain unexplained. These issues are considered fundamental and would require major methodological restructuring rather than incremental revision. I therefore recommend rejection of the manuscript in its present form. Specific comments are provided below to clarify the main concerns and to explain in more detail the basis for this recommendation.

The authors thank the reviewer for the detailed comments and thoughtful suggestions, which are very helpful in improving the manuscript. We have carefully considered all the comments and revised the manuscript accordingly. A detailed point-by-point response to these comments is presented below.

1. L47: "However, existing aerosol retrievals based on DPC observations have primarily focused on AOD." This statement is not valid. A large number of studies have already used DPC observations to retrieve aerosol optical properties beyond AOD.

We thank the reviewer for this correction. We agree that several studies have already retrieved aerosol optical properties beyond AOD from DPC observations using physical inversion methods and machine learning approaches. Our original statement was not sufficiently precise. Our intention was to emphasize that SSA retrievals specifically from DPC/GaoFen-5 observations, especially at global scales, remain relatively limited, and the currently available studies still have constraints (e.g., regional scope, surface-type limitation, or limited SSA accuracy).

To make this clear, we revisited the relevant literature and revised the text accordingly. Specifically, (1) Dong et al. (2024) retrieved SSA using a machine-learning approach, but the retrieval is limited to land conditions; (2) Fang et al. (2022) reported regional SSA retrieval rather than global SSA; and (3) Jin et al. (2024), Ji et al. (2025), and Zhang et al. (2025) reported SSA retrievals based on DPC-2/GaoFen-5(02) observations. Because DPC-2/GaoFen-5(02) differs from DPC/GaoFen-5 in instrument design and in temporal coverage, these results are not directly comparable to SSA retrieval from DPC/GaoFen-5, and therefore do not resolve the limited evidence for global SSA retrieval based on DPC/GaoFen-5 observations.

Based on this survey, we have revised the expression in L47-58 to avoid suggesting that DPC-based retrievals focus only on AOD, while correctly stating that SSA retrievals from DPC/GaoFen-5 remain less reported at global scales:

> *Many aerosol retrieval studies based on DPC/GaoFen-5 observations have reported high-quality AOD retrievals (with correlation coefficients up to 0.9 against ground-based measurements). Several studies have also extended the retrieval to additional aerosol optical properties, including SSA…Nevertheless, compared with AOD, SSA retrievals based on DPC/GaoFen-5 observations have been less frequently reported at large spatial scales, and studies that provide global SSA retrieval remain relatively limited.*

2. L55: "while numerical methods have so far been limited to regional and oceanic applications." This statement is not correct. DPC observations have already been used to retrieve aerosol parameters over land and at the global scale. Please add recent references related to aerosol retrievals using DPC observations. In addition, "This highlights the need for further exploration of global SSA retrieval using DPC observations" is also not valid, as global SSA retrievals based on physical methods and DPC observations have already been reported.

We thank the reviewer for this correction. We agree that our original expression was not accurate. Physically based numerical inversion methods using DPC observations have been applied for global aerosol retrievals (especially for AOD). Our intention was to emphasize

that, compared with AOD, global-scale SSA retrievals from DPC based on physical methods are still relatively limited, and existing studies often focus on specific regions or over ocean.

After re-checking the recent literature, we found that while global aerosol retrievals from DPC observations using physical methods have indeed been reported (primarily focusing on AOD and related parameters), we did not identify a clearly documented study that performs global SSA retrieval using a physically based inversion method specifically with DPC/GaoFen-5 observations. Some global SSA retrieval studies exist but are based on different sensors. For example, Zhang et al. (2025) implemented the RemoTAP method for global SSA retrieval over land, but it was conducted using DPC-2/GaoFen-5(02) data rather than DPC/GaoFen-5. Given differences in instrument design and temporal coverage, those results are not directly comparable to a global SSA retrieval based on DPC/GaoFen-5 observations.

Therefore, we revised the text in L57-59 to remove the misleading statement and to avoid implying that global SSA retrievals do not exist:

> *On the other hand, studies applying physically based inversion methods to DPC observations for global SSA retrieval are still relatively limited. Further efforts are therefore needed to extend such physically based approaches on the global scale.*

3. L63: "This study uses measurements from the first DPC sensor since data is not well calibrated for the following two sensors." This statement is unclear. Which sensor is referred to as the "first DPC sensor"?

We thank the reviewer for pointing it out. In this study, the "first DPC sensor" refers to the DPC instrument onboard the Gaofen-5 satellite launched in May 2018. We have revised the manuscript in L70 to clarify:

> *This study uses measurements from the DPC instrument onboard the Gaofen-5 satellite launched in May 2018, as the data from the subsequent DPC instruments onboard Gaofen-5(02) and Daqi-1 are not yet well calibrated.*

4. L68: What do you mean by "instrumental drift" in this context?

Thank you for the comment. In this study, "instrumental drift" refers to a gradual change in the radiometric response of the DPC sensor after launch. This drift is mainly attributed to aging and degradation of the optical system in the space environment, rather than changes in the detectors. As a result, the measured TOA radiance for the same target can slowly shift over time, leading to increasing radiometric biases if no correction is applied. This drift is known to be dependent on both wavelength and field of view (FOV, or viewing geometry), with a stronger sensitivity decrease at shorter wavelengths and larger variations across the FOV, as reported by Zhu et al. (2022). We have revised the expression in the manuscript in L79-81 to clarify:

> *However, after launch, DPC exhibited a gradual change in radiometric sensitivity, primarily due to aging of the optical components. This drift is dependent on both wavelength and field of view and can introduce increasing systematic biases if not properly corrected.*

5. L70: What does "Rayleigh scattering-based" refer to?

Thank you for this comment. The term "Rayleigh scattering-based" refers to a radiometric calibration method developed by Zhu et al. (2022) which is based on the atmospheric Rayleigh scattering over deep ocean regions. In these areas with very low aerosol loading and low surface reflectance, the TOA radiance observed by the satellite is dominated by Rayleigh scattering, which can be accurately simulated using a Radiative Transfer Model (RTM). Zhu et al. (2022) quantified differences of DPC observed and RTM simulated radiances over these deep ocean regions, and derived monthly VZA-dependent calibration coefficients. In this study, these coefficients are applied to correct DPC radiance observations in order to reduce radiometric biases before aerosol and surface property retrievals. We have revised the manuscript to better describe the calibration procedure in L82-89.

> *The radiometric response of DPC/GaoFen-5 is progressively drifting over time and is realted to VZA. Zhu et al. (2022) developed a method based on Rayleigh scattering over the ocean to correct this drift. In deep ocean regions with very low aerosol loading and low surface reflectance, the TOA radiance observed by*

satellite sensors is dominated by atmospheric Rayleigh scattering, which can be accurately simulated using radiative transfer models. By comparing simulated radiances with DPC observations over such regions, Zhu et al. (2022) provided monthly VZA-dependent calibration coefficients at 443, 490, 565, and 670 nm. The calibration uncertainties are about 1-7 % (depending on the wavelength and VZA). In this study, these Rayleigh scattering-based calibration coefficients are applied to correct DPC's scalar reflectance at 443, 490, 565, and 670 nm.

6. L76–77: "the screening of cloud/ice/snow pixels additionally employs the original measurements from the other bands." Why are uncalibrated measurements used for cloud/ice/snow screening? You mentioned that the uncertainty of DPC observations may exceed 20%. Please quantify the retrieval errors introduced by not using calibration coefficients. You did not specify which calibration coefficients were used for the polarization measurements. First, please clearly state whether calibration coefficients were applied and provide their values. Second, if no calibration coefficients were used, please quantitatively assess the retrieval errors caused by ignoring calibration.

Thank you for this comment. We clarify that radiometric calibration was applied only to the scalar reflectance of the four retrieval bands (443, 490, 565, and 670 nm), because existing calibration studies for DPC/ GaoFen-5 have so far provided coefficients only for these four bands. For the other scalar bands and for all polarization observations, calibration coefficients were not applied because reliable post-launch calibration information (including coefficients) is currently unavailable.

The cloud/ice/snow screening also relies on the 865 nm observations as well as polarimetric reflectance, and these inputs therefore come from the original (uncalibrated) measurements. We acknowledge that uncalibrated data may affect screening performance, leading to either over-screening or residual cloud contamination. To reduce the risk of retaining cloudy pixels, we adopted more conservative thresholds. For example, given that the uncertainty at 865 nm can be as large as ~23%, we increased the screening threshold by 20%. Over land, the criterion (R_{865}/R_{443}) was adjusted from 1.2 to 1.44. This tightening is intended

to maintain robust cloud removal even when the uncalibrated 865 nm reflectance is positively biased.

Finally, the impact of ignoring calibration is mainly indirect because the retrieval itself uses only the four calibrated scalar bands. The resulting error is introduced through screening, i.e., by changing the balance between residual cloud contamination and the loss of valid clear pixels.

7. L92: "The AOD measurements can be obtained at several wavelengths ranging from 340 nm to 1640 nm." AERONET does not appear to provide AOD measurements at 1640 nm.

Thank you for the comment. AERONET does provide AOD measurements at 1640 nm for sites equipped with Cimel sun photometers that include an InGaAs detector. As described by Giles et al. (2019), the nominal standard AERONET aerosol wavelengths include 340, 380, 440, 500, 675, 870, 1020, and 1640 nm. The availability of the 1640 nm channel depends on the instrument configuration at a given site, and therefore not all AERONET stations provide measurements at this wavelength.

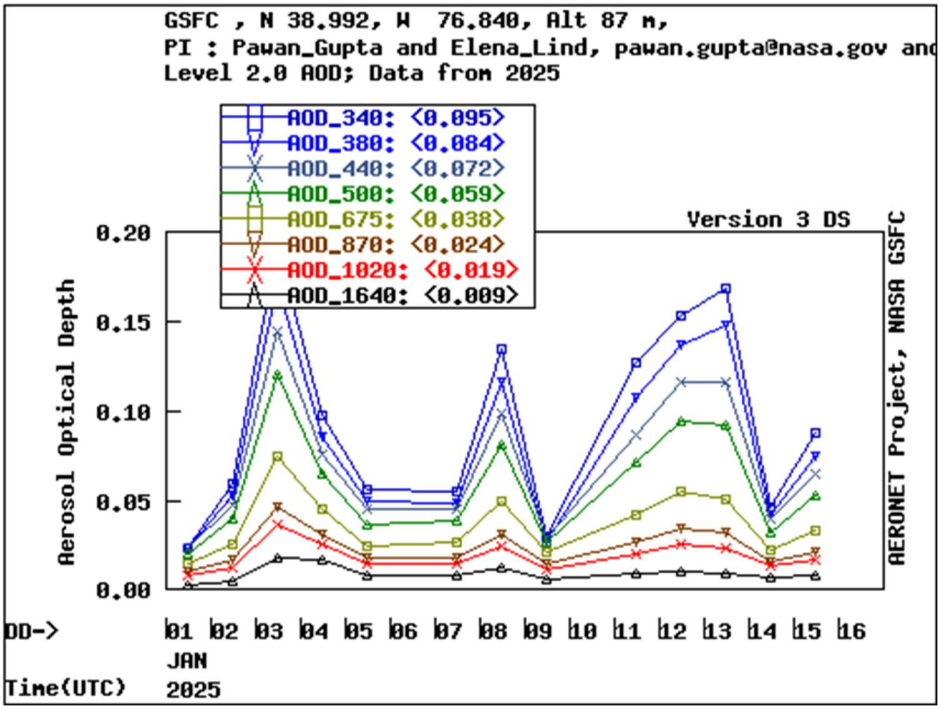

Fig. R1-1. AERONET Level 2.0 daily AOD observations at the GSFC site for January 2025. The figure is provided by NASA, downloaded from https://aeronet.gsfc.nasa.gov/ on 6 February 2026.

As an illustration, Fig. R1-1 shows Level 2.0 AOD data for January 2025 from the AERONET GSFC site (downloaded from the AERONET website), which include valid observations at 1640 nm. We agree that the original wording may imply that all AERONET sites provide AOD at 1640 nm, and we have revised the manuscript in L105 to clarify:

> *The AOD measurements are available at multiple wavelengths ranging from 340 to 1640 nm, depending on the site and instrument configuration, whereas the SSA products are provided at four wavelengths at 440, 675, 870 and 1020 nm.*

8. L96–97: "we utilize the all-point Version 3 Level 2.0 direct AOD measurements." This statement is unclear. Does "direct AOD" mean that the AOD is not quality-controlled? What does "all-point" refer to?

Thank you for the comment. The "direct AOD" refers to aerosol optical depth retrieved from direct-sun observations of the AERONET sun photometer, as opposed to AOD products derived from sky-radiance inversions. It does not indicate that the data are unprocessed. The Version 3 Level 2.0 AERONET AOD data used here have undergone standard cloud screening and quality control.

The term "all-point" refers to the original temporal resolution of the AERONET observations, i.e., individual measurement points for each observation time. The "all-point" data is a product provided by AERONET, in contrast to those temporally aggregated products such as daily-mean or monthly-mean data.

We have revised the manuscript in L109-112 to clarify:

> *Considering the data quality and data availability, this study utilizes the Version 3 all-point (individual measurement) Level 2.0 AERONET AOD data derived from direct-sun observations, along with quality-controlled Level 1.5 almucantar SSA retrievals from sky radiance measurements.*

9. In Eq. (4), the cost function of the retrieval algorithm is given, but the state vector to be retrieved and the prior information are not specified.

Thank you for this comment. We agree that the state vector and the prior information should be specified. In the revised manuscript, we have clarified the composition of the state vector, a priori estimates, and the associated errors in Sect. 2.6.

Specifically, the state vector has been described as a combination of aerosol and surface parameters (L180-189):

> *The state vector, $\boldsymbol{x}$, is composed of aerosol and surface parameters. Particularly, for land surfaces, the state vector $\boldsymbol{x}$ consists of AOD ($\tau(\lambda)$), SSA ($\omega(\lambda)$), kernel intensity parameters of RTLS model ($K(\lambda)$, k_{vol}, and k_{geo} in Eq. 2), and the scale factor of BPDF-NDVI model (C in Eq. 8)…For water surfaces, only $\tau(\lambda)$ and $\omega(\lambda)$ are retrieved as components of the state vector $\boldsymbol{x}$, and the New Cox-Munk model is implemented to compute the surface reflectance (Spurr, 2006). The wavelength-dependent parameters, $\tau(\lambda)$, $\omega(\lambda)$, and $K(\lambda)$, are retrieved at 443, 490, 565, and 670 nm, corresponding to the wavelengths at which DPC observations are used to construct the measurement vector.*

The description of a priori values and the corresponding uncertainties has also been clarified in L189-192:

> *For AOD and SSA, the a priori state vector and its associated error covariance matrix are prescribed as fixed values, derived from the mean and variance of AERONET measurements. The a priori estimates of surface properties are also fixed, with their errors defined by the corresponding ranges of variability.*

We have also added a table (Table 3) summarizing the state vector and the associated prior information.

10. Section 3.1: What SSA value is used in the simulations? Under different SSA conditions, a ±0.03 perturbation may lead to completely different conclusions. Moreover, the apparent reflectance change induced by SSA perturbations does not seem equivalent to the accuracy required for satellite aerosol retrievals.

Thank you for this comment. In the original manuscript, the SSA used in Sect. 3.1 was computed using a Mie code (Mishchenko et al., 1999), based on the refractive index and

particle size distribution of the moderately absorbing aerosol type (Levy et al., 2007). Specifically, the baseline SSA decreases slightly with wavelength, from 0.94 at 443 nm to 0.92 at 865 nm, and the sensitivity tests in Sect. 3.1 were conducted by perturbing SSA around this spectral baseline.

In the revised manuscript, we expanded the SSA range to 0.8-1.0. We also examined whether the same SSA perturbation produces comparable changes in I and DOLP at different SSA levels (Fig. R1-2). The results show that changing SSA from 0.8 to 0.84 (Fig. R1-2a,b) and from 0.96 to 1.0 (Fig. R1-2c,d) leads to broadly similar variations in I and DOLP. Therefore, under different SSA conditions, the impacts of the same perturbation are likely to be similar.

We also agree that the current observation accuracy is not sufficient to resolve the small changes in I and DOLP induced by 0.03 SSA perturbations. As a result, SSA retrievals based on DPC measurements can have large uncertainties, which is consistent with the relatively large errors reported in existing SSA products.

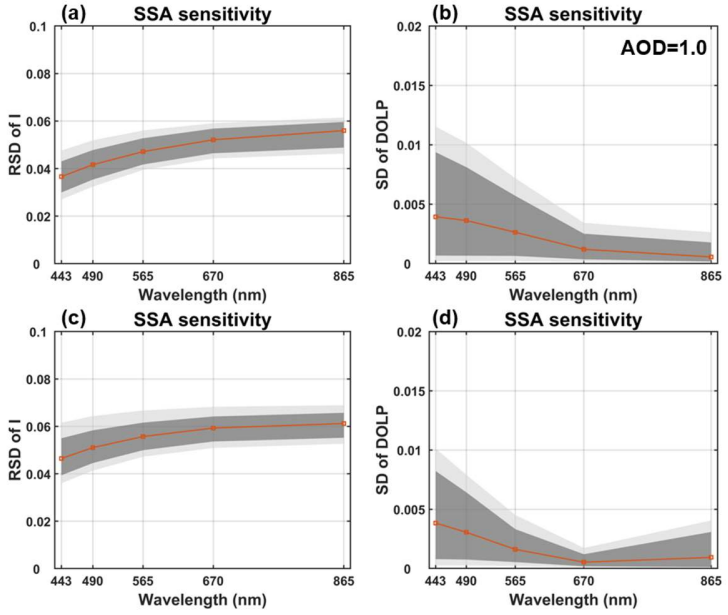

Fig. R1-2. Relative standard deviation (RSD) of I (a, c) and standard deviation (SD) of DOLP (b, d) induced by variations in SSA under different SSA levels. SSA varies from 0.80 to 0.84 in (a, b), and from 0.96 to 1.00 in (c, d).

11. In Fig. 5, please explain why AOD and DHR are simultaneously underestimated under high aerosol loading conditions. In addition, why do the numbers of retrieved AOD values differ among different wavelengths?

Thanks for this insightful comment. The underestimation observed under high aerosol loading conditions is not strictly simultaneous between AOD and DHR. By shading the AOD retrievals according to the DHR residual (Fig. R1-3(a)), we find that in part of the underestimated high-AOD cases, the retrieved DHR are overestimated, suggesting a compensation effect between surface reflectance and aerosol loading within the inversion framework. In addition, the AOD retrieval is also coupled with SSA. Under high aerosol conditions, underestimated AOD frequently corresponds to overestimated SSA (Fig. R1-3(b)), further reflecting parameter trade-offs in the retrieval process. Finally, the presence of residual errors in the retrieval is expected.

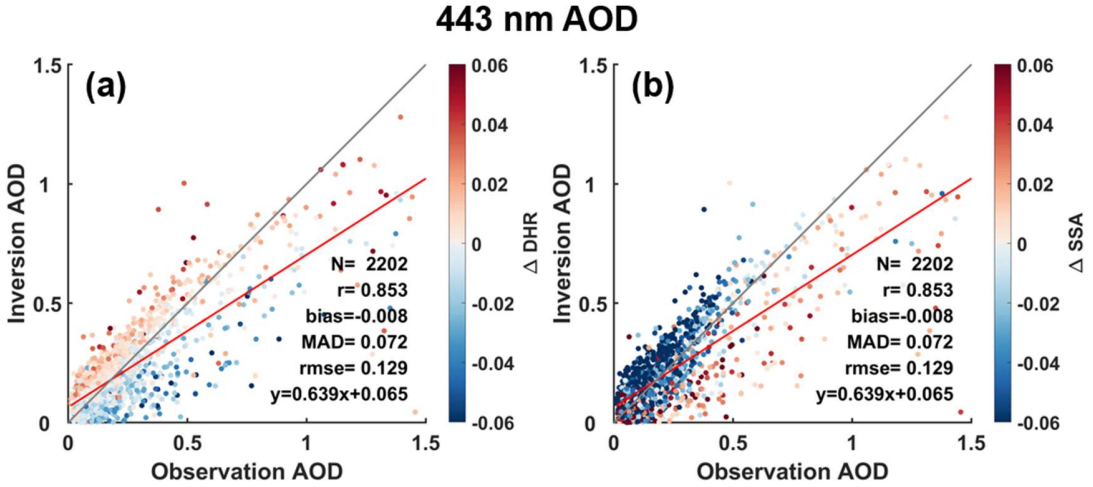

Fig. R1-3. Validation results of AOD at 443 nm. The points are shading to the (a) DHR residual (ΔDHR), and (b) SSA residual (ΔSSA).

As for the differing numbers of retrieved AOD values among wavelengths, this discrepancy originates from the previous quality control procedure based on single bands. In the original implementation, each wavelength was screened independently based on whether the retrieved parameters fell within the predefined ranges listed in Table 3. Retrievals located at the preset boundaries were regarded as less reliable and excluded, resulting in band-dependent sample sizes. In the revised manuscript, we have adopted a joint quality

control strategy that evaluates all wavelengths involved in the inversion simultaneously, ensuring consistent sample selection across bands.

12. In Fig. 8, the map of AOD contains missing values, while SSA does not. Why?

We thank the reviewer for pointing this out. The missing values in the AOD map of Fig. 8 are mainly associated with cloud patches, which were correctly screened in the map of AOD. After careful examination, we found that during the spatial resampling step of the SSA image processing, these masked grids were not properly excluded due to a processing issue. This issue has been identified and fixed, and Fig. 8 has been updated accordingly in the revised manuscript.

13. Under biomass burning conditions, why do high SSA values overlap with possible aerosol plumes? Biomass burning is generally expected to emit strongly absorbing aerosols. Please explain.

We thank the reviewer for this important comment. Biomass burning aerosols are generally characterized by enhanced absorption and relatively low SSA. After carefully comparing the true-color image, AOD map, and SSA map, we note that the relatively high SSA values are mainly located at the edges of the smoke plumes, where AOD is comparatively low, rather than in the core areas of the plumes. On one hand, under low-AOD conditions, SSA retrieval becomes less constrained and exhibit higher uncertainty, and the solution is more sensitive to the assumed initial values. The SSA values in these regions (approximately 0.92–0.95) might be influenced by the selected initial settings. On the other hand, the SSA values in these regions are typically around 0.92–0.95, which does not indicate strongly scattering aerosols but rather moderate absorption. This is also consistent with possible mixing and aging effects near plume edges, which may increase SSA relative to the fresh plume core. This is in line with in situ observations reported by Kleinman et al. (2020), who found that near-fire aerosol had SSA of ~0.8-0.9, while after ~1-2 hours of aging SSA was typically ~0.9 or higher. We have clarified this point in the revised manuscript in L377:

The relatively higher SSA values are mainly located at the edges of the biomass-burning plumes, where AOD is relatively low and the SSA retrieval has larger uncertainty. In these regions, the retrieved SSA (typically around 0.92–0.95) is

weakly constrained and therefore more sensitive to the assumed a priori values. Such SSA values suggest moderately absorbing aerosols and may reflect the influence of possible mixing and aging processes near the plume edges, consistent with Kleinman et al. (2020), who reported that near-fire smoke had SSA of ~0.8-0.9, while after ~1-2 h of aging SSA was typically ~0.9 or higher.

To mitigate this issue, future improvements of the retrieval algorithm will consider incorporating spatiotemporal constraints to better stabilize SSA retrievals in such regions.

14. Fig. 9 shows similar issues to Fig. 8. The missing values of AOD and SSA do not overlap. In addition, irregular blank areas appear in coastal regions. Please explain the reasons.

We thank the reviewer for the comment. The missing values of AOD and SSA do not overlap because of the quality-control criteria applied to SSA. In particular, SSA retrievals are unreliable under low AOD conditions. Therefore, SSA values are screened when AOD falls below a predefined threshold (AOD<0.3), whereas the corresponding AOD values are retained. This explains the larger number of missing values in the SSA map, which are predominantly located in regions with low AOD.

The irregular blank areas in coastal regions have a different origin. In our retrieval, land and ocean pixels are treated using different surface parameterizations. However, coastal pixels cannot be clearly classified as either land or ocean under the current surface treatment. To avoid introducing large surface-related biases, these coastal pixels are excluded from the retrieval, resulting in irregular blank areas near coastlines.

We have also revised the manuscript in L387 to clarify:

Coastal pixels are excluded from the retrieval because they cannot be clearly classified as land or ocean, leading to missing values near coastlines. SSA values in low-AOD regions are also screened due to low reliability.

15. Please explain the anomalously high AOD values at high latitudes in Fig. 10(c) and over northwestern China in Fig. 10(d).

We thank the reviewer for this comment. By examining the retrieval results and true-color imagery for the corresponding periods, we found that these anomalously high AOD values are likely attributed to residual cloud contamination that was not completely removed by the cloud screening process. Particularly, in January 2020 (Fig. 10(d)), the affected regions show persistent, widespread thick cloud cover. In October 2019 (Fig. 10(c)), cloud cover is also frequently observed at high latitudes. This increases the likelihood of cloud contamination and can lead to artificially high AOD. In the revised manuscript, we have applied a more rigorous cloud screening procedure to better suppress these cloud-related artifacts, and the corresponding figures have been updated accordingly.

16. Please explain the anomalously low SSA values over South America in Fig. 11(b) and over northern Asia in Fig. 11(c).

We thank the reviewer for this comment. The reason is the same as in the previous comment: the anomalously low SSA values are most likely related to residual cloud contamination. In the revised manuscript, we have applied a more rigorous cloud screening procedure, which reduces these low-SSA artifacts over South America (Fig. 11(b)) and northern Asia (Fig. 11(c)), and the figures have been updated accordingly.

17. Please add comparisons with other satellite aerosol products and provide global difference maps.

We thank the reviewer for this comment. In the revised manuscript, we have added regional MODIS AOD map during the pollution event in the manuscript. In addition, monthly global MODIS AOD maps and the corresponding global difference maps are provided in the Supplement. Related analysis and discussions have also been added into Sects. 3.4 and 3.5 to further evaluate our results.

18. Please explain the reason why AOD and DHR are simultaneously underestimated under high aerosol loading conditions.

Thank you for this comment. The underestimation under high aerosol loading is not strictly simultaneous between AOD and DHR. Analysis based on DHR differences indicates that, in part of the underestimated high-AOD cases, DHR is overestimated, suggesting a

compensation effect between surface reflectance and aerosol loading within the inversion. Moreover, underestimated AOD under heavy aerosol conditions is often accompanied by overestimated SSA, further reflecting parameter trade-offs in the retrieval framework. A more detailed discussion is provided in our response to Comment #11.

19. Please correct the grammatical errors throughout the manuscript.

We thank the reviewer for this comment. We have carefully checked the manuscript and corrected the grammatical errors.

Reference

Dong, Y., Li, J., Zhang, Z., Zheng, Y., Zhang, C., & Li, Z. (2024). Machine learning-based retrieval of aerosol and surface properties over land from the gaofen-5 directional polarimetric camera measurements. *IEEE Transactions on Geoscience and Remote Sensing*, *62*, 1–15. https://doi.org/10.1109/tgrs.2024.3419169

Fang, L., Hasekamp, O., Fu, G., Gong, W., Wang, S., Wang, W., et al. (2022). Retrieval of aerosol optical properties over land using an optimized retrieval algorithm based on the directional polarimetric camera. *Remote Sensing*, *14*(18), 4571.

Giles, D. M., Sinyuk, A., Sorokin, M. G., Schafer, J. S., Smirnov, A., Slutsker, I., et al. (2019). Advancements in the aerosol robotic network (AERONET) version 3 database automated near-real-time quality control algorithm with improved cloud screening for sun photometer aerosol optical depth (AOD) measurements. *Atmospheric Measurement Techniques*, *12*(1), 169–209. https://doi.org/10.5194/amt-12-169-2019

Ji, Z., Li, Z., Zhang, Z., Fu, G., Hasekamp, O., Fan, C., et al. (2025). Retrieval of aerosol properties over the ocean using data from the second-generation directional polarization camera (DPC-2) onboard the GF-5(02) satellite. *Journal of Geophysical Research: Atmospheres*, *130*(17). https://doi.org/10.1029/2025jd043908

Jin, S., Ma, Y., Wang, Z., Hong, J., Chen, F., Ti, R., et al. (2024). Retrievals and performance assessment of global marine aerosol optical properties from DPC/GRASP. *Journal of Atmospheric and Environmental Optics*, *19*(6), 680–697.

Kleinman, L. I., Sedlacek III, A. J., Adachi, K., Buseck, P. R., Collier, S., Dubey, M. K., et al. (2020). Rapid evolution of aerosol particles and their optical properties downwind of wildfires in the western US. *Atmospheric Chemistry and Physics*, *20*(21), 13319–13341. https://doi.org/10.5194/acp-20-13319-2020

Levy, R. C., Remer, L. A., & Dubovik, O. (2007). Global aerosol optical properties and application to moderate resolution imaging spectroradiometer aerosol retrieval over land. *Journal of Geophysical Research: Atmospheres*, *112*(D13), D13210. https://doi.org/10.1029/2006jd007815

Mishchenko, M. I., Dlugach, J. M., Yanovitskij, E. G., & Zakharova, N. T. (1999). Bidirectional reflectance of flat, optically thick particulate layers: An efficient radiative transfer solution and applications to snow and soil surfaces. *Journal of Quantitative Spectroscopy and Radiative Transfer*, *63*(2-6), 409–432. https://doi.org/10.1016/s0022-4073(99)00028-x

Spurr, R. J. D. (2006). VLIDORT: A linearized pseudo-spherical vector discrete ordinate radiative transfer code for forward model and retrieval studies in multilayer multiple scattering media. *Journal of Quantitative Spectroscopy and Radiative Transfer*, *102*(2), 316–342. https://doi.org/10.1016/j.jqsrt.2006.05.005

Zhang, Z., Li, Z., Fu, G., Hasekamp, O., Fan, C., Qie, L., et al. (2025). Global aerosol retrieval over land using the chinese satellite polarimeter DPC-2/GF-5(02). *IEEE Transactions on Geoscience and Remote Sensing*, *63*, 1–14. https://doi.org/10.1109/tgrs.2025.3633391

Zhu, S., Li, Z., Qie, L., Xu, H., Ge, B., Xie, Y., et al. (2022). In-flight relative radiometric calibration of a wide field of view directional polarimetric camera based on the rayleigh scattering over ocean. *Remote Sensing*, *14*(5), 1211. https://doi.org/10.3390/rs14051211

Report 2

Reply to Anonymous Referee #1

This article develops a numerical method for simultaneously retrieving AOD, SSA and DHR from DPC multi-angle polarimetry (MAP) observations. The authors analyze the sensitivities of both scalar and polarimetric reflectance to SSA, and get reliable results of global AOD, SSA, and DHR based on the retrieval algorithm. As one of the few operational spaceborne MAP sensors, inversion algorithms based on DPC observations, particularly those for SSA retrieval, remain quite limited, with few global SSA products currently available. This study provides a reference for the design of future MAP sensors and the development of aerosol retrieval algorithms. The global SSA maps presented in this article also provide valuable insights into aerosol scattering and absorption characteristics in recent years. However, several aspects of the data, methods, and results require further clarification and improvement.

We thank the reviewer for the detailed comments and thoughtful suggestions, which are very helpful in improving our manuscript. We have carefully addressed all concerns and revised the manuscript accordingly. A point-by-point response is presented below.

General comments:

2. Data used in the article: The authors retrieve aerosol and surface parameters from DPC measurements, and validate the retrieved results according to comparing with AERONET and MODIS products. However, there are several points need to be clarified. (1) DPC data: The description of DPC data is not very clear. The authors introduce that DPC provide observations across 8 spectral bands, but only 5 bands are mentioned in Section 2.1. Moreover, the use of polarized observations is also not specified. (2) AERONET data: The authors use all the Level 2.0 quality control criteria except AOD threshold to screen the AERONET Level 1.5 SSA. But the 0.4 AOD threshold are still utilized to screen the SSA in the validation progress. Why not directly utilize the Level 2.0 SSA data? (3) The periods of DPC and AERONET data used in the article are not specified.

We thank the reviewer for the suggestion about the usage of data in the article.

(1) DPC data: We have revised the manuscript and listed all the DPC channels in L73:

The sensor provides measurements across 8 spectral bands (443, 490, 565, 670, 763, 765, 865, and 910 nm) from visible to near-infrared wavelengths.

The use of DPC observations have been listed in Table 2 and clarified in L167:

The measurement vector, $\boldsymbol{y}$, is constructed with calibrated scalar reflectance at 443, 490, 565, and 670, as well as DOLP at 490 and 670 nm from several angles.

(2) AERONET data.

Although AERONET Level 2.0 SSA data provide the highest quality, the number of available Level 2.0 SSA retrievals during the study period (6 months) is very limited, which would not allow a statistically meaningful validation of the algorithm performance. In order to balance the data quality and data availability, all Level 2.0 quality control criteria except for the AOD threshold were applied to the Level 1.5 data. Moreover, the AOD threshold ($\mathrm{AOD}_{440} > 0.4$) was applied only in the SSA validation step and was based on the retrieved AOD, rather than the AERONET AOD. This filtering was introduced to exclude cases with insufficient sensitivity of the measurements to SSA, and it was not applied to the validation of AOD or DHR. Therefore, quality-controlled AERONET Level 1.5 data were used in this study.

(3) Periods of data:

We thank the reviewer for pointing out this missing information. In the revised manuscript, we have explicitly specified the time periods of both the DPC and AERONET data used in this study. Six months of DPC Level 1 data, covering April, July, and October 2019, as well as January–March 2020, are used for the retrieval. The AERONET observations used for validation correspond to the same periods as the DPC overpasses. This information has been added in L75:

Six months of DPC Level 1 data, encompassing April, July, and October 2019, as well as January-March 2020, are used in the retrieval in this study. The AERONET, MODIS, as well as other auxiliary data are selected from the same periods.

3. Retrieval algorithm: The authors have provided a detailed description of the retrieval algorithm, but the introduction to the flowchart could be strengthened by providing more details. The authors can consider the following aspects. (1) The DPC observations have "up to 12 viewing angles" and typically "exceeding 9 angles". Are observations from all the angles used for inversion? What about those pixels with viewing angles less than 9? (2) Which method is employed to minimize the cost function? (3) What criteria are utilized for the matching of DPC and AERONET data?

We thank the reviewer for the suggestion about the retrieval algorithm in the article.

(2) In this study, only pixels with at least 9 valid viewing angles were used for the inversion. Pixels with fewer than 9 viewing angles, which are primarily located near the scan edges, were excluded to ensure sufficient angular sampling. For the remaining pixels, observations from the first 9 viewing angles were used for the retrieval to maintain a consistent angular configuration across all pixels. We have added the relevant description in the manuscript in L170:

However, most pixels are observed from more than 9 viewing angles. Pixels with fewer than 9 viewing angles, which are primarily located near the scan edges, were therefore excluded. For the remaining pixels, observations from the first 9 viewing angles were used in the retrieval to maintain a fixed number of viewing angles for all pixels. Consequently, the scalar reflectance and DOLP at each wavelength consist of measurements acquired from 9 viewing angles.

(3) In this study, the cost function is minimized using an iterative Gauss–Newton method. This information has been added to the revised manuscript in L201:

The algorithm minimizes the cost function defined in Eq. 4 using an iterative Gauss–Newton method to obtain the final retrieval results.

(4) In the numerical simulation experiments, daily AERONET data are used to describe representative aerosol parameters, and a spatial collocation radius of 8 km is used. We have added the relevant description in the manuscript in L223:

The simulated dataset was constructed using aerosol parameters derived from daily AERONET observations selected within an 8 km radius of DPC overpass locations to represent typical aerosol conditions observed by DPC. The corresponding viewing geometry, including SZA, VZA, and RAA, was taken from the matched DPC observations and used in the radiative simulations, thereby accounting for the actual scattering angle distribution of DPC observations.

4. Validation results: The authors analyzed several statistical indicators (e.g., correlation coefficient, RMSE, bias) to validate retrieval results. For SSA validation, the ratio of points falling within the Error Envelope (EE) is also a useful indicator to assess the result. It would be helpful to add EE lines to the figures and annotate the corresponding point ratios.

Thanks for the very helpful suggestion. We have added the ± 0.03 Error Envelope (EE) lines to the SSA validation scatter plot and indicated the proportion of samples falling within the EE in the figure. Corresponding analysis has also been added in the manuscript.

5. Global maps: Section5 shows global retrieval results. These maps provide valuable insights into aerosol and surface properties. I have two comments about these results. (1) The authors explain that the zonal discontinuities in the maps are primarily due to defects in the original data. However, the discontinuities observed over oceanic areas also seems to be related to the incompletely filtered clouds. Would be better to clarify in the manuscript. (2) Heavy AOD is observed over Southern Oceans in January 2020. The authors attributes it to the strong Australian wild fires. However, the AOD over Southern Oceans almost reaches 0.5 in Fig. 10(d). Is this magnitude reasonable? Was it also observed by other sensors?

We thank the reviewer for the helpful comments.

(3) We agree that the zonal discontinuities observed over oceanic regions may also be related to incompletely filtered clouds, in addition to defects in the original data. In

this study, cloud screening also relies on observations at 865 nm, which have not been re-calibrated and can have higher uncertainties (up to about 23%). As a result, cloud pixels may not be completely removed. We have revised the manuscript to clarify this limitation and added a discussion acknowledging that residual cloud effects related to the cloud screening procedure may contribute to the observed discontinuities.

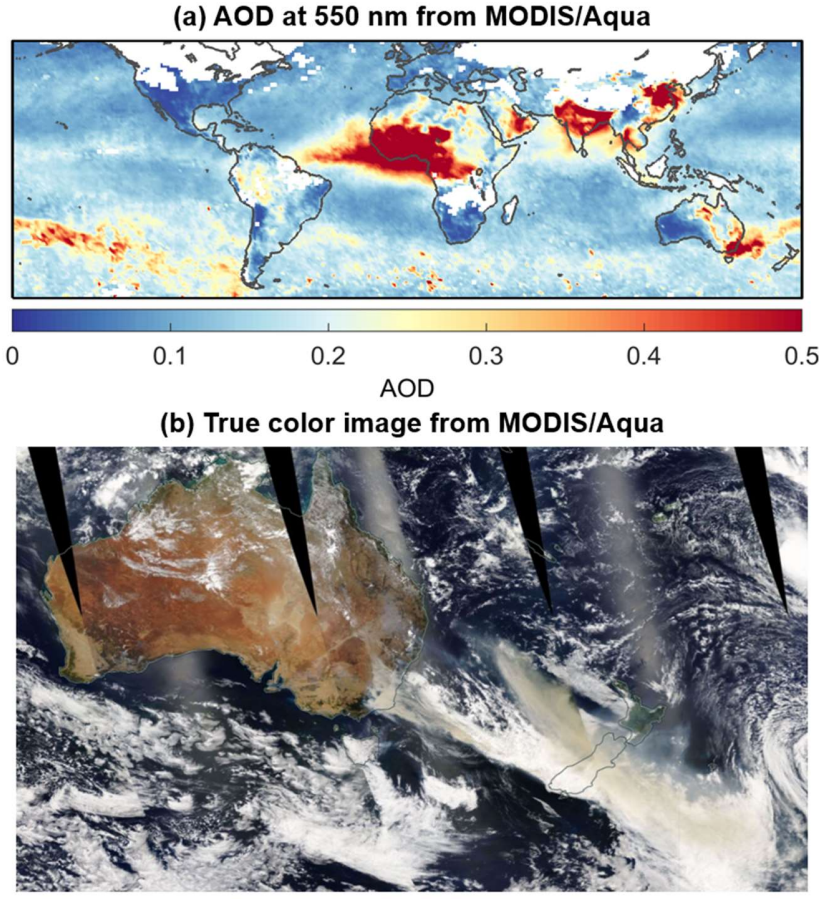

Fig. R2-1. (a) Global AOD for January 2020 at 550 nm from MODIS/Aqua Level 3 product. (b) True color image from MODIS/Aqua on January 1, 2020.

(4) As for the abnormally high AOD values observed over the Southern Ocean, we conducted further examinations using true-color imagery and MODIS AOD products. The true-color imagery (Fig. R2-1b) for early January 2020 reveals extensive smoke plumes over the Southern Ocean originating from southeastern Australia and gradually transported eastward. This indicates that large amounts of

biomass-burning aerosols were present over the region during this period. The MODIS monthly AOD product for January 2020 also shows anomalously high AOD over the Southern Ocean, with values exceeding 0.5 in some areas (Fig. R2-1a). The spatial pattern and magnitude are generally consistent with our retrieval results. Thus this magnitude is likely reasonable. We have added the corresponding MODIS AOD map to the Supplement material, and included a relevant discussion in the manuscript in L440:

The anomalously high AOD over the Southern Ocean in January 2020 reaches values of up to 0.5 in some regions, consistent with independent data sources (e.g., MODIS AOD, see Supplement).

Minor comments:

3. L68: The calculation of DOLP is not described in the article.

Thanks for reminding. We have added an equation (Eq. 7) of calculating DOLP in the manuscript in Sect. 2.6.

4. Fig. 2-4: Please explain the x label "scat_ang" in the caption.

Thanks for reminding. The xlabel "scat_ang" refers to "scattering angle", and we have explained in the caption of Fig. 2.

5. Fig. 7: DHR data are not AERONET observations. Please revise the caption.

Thanks for reminding. We have revised the caption of Fig. 7 to clarify the data sources:

Comparison between retrieved AOD (left) and SSA (middle) at 443 nm and AERONET observations, and comparison between retrieved DHR (right) at 443 nm and the MODIS product.

6. Section 3.2: Please keep the number of significant digits consistent.

Thanks for pointing it out. We have carefully checked Section 3.2 and revised the manuscript to ensure that the number of significant digits is used consistently throughout this section.

6. Fig. 8: The “(a)/(b)/(c)” labels are not marked in the figures.

Thanks for reminding. We have added labels in Figs. 8 and 9.

7. Figs. 8-12: The wavelength labeled in the figures (440 nm) does not match the wavelength mentioned in the text (443 nm). Please update either the figures or the relevant text for consistency.

Thanks for pointing out this inconsistency. The wavelength labels have been carefully checked and updated for consistency. All references have now been unified to 443 nm in both the figures and the corresponding text.

Report 3

Reply to Anonymous Referee #4

General comments:

This manuscript presents the simultaneous retrieval of aerosol optical depth (AOD), single scattering albedo (SSA) and directional-hemispheric reflectance (DHR) from the Directional Polarimetric Camera (DPC) aboard China's Gaofen-5 satellite. The sensitivity analysis, performance evaluation by synthetic data, and application to actual DPC data are discussed. The sensitivity analysis demonstrates the challenges in retrieving SSA values from the DPC data, while the algorithm based on optimal estimation is designed to overcome the challenges. The performance of the developed algorithm is evaluated both based on synthetic data and Aerosol Robotic Network (AERONET) data. A case study and global maps are also presented. While this manuscript covers a very challenging topic and takes a conservative approach, the restrained reproducibility and incomplete analysis limit the value of this manuscript to the research community. The manuscript would require a substantial revision for final publication in AMT if authors are willing to do so. The following points should be addressed to increase the impact of this manuscript.

We appreciate the reviewer for the constructive comments and thoughtful suggestions, which are very helpful in improving our manuscript. We have carefully considered all the comments and revised the manuscript accordingly. Below is a detailed point-by-point response to these comments.

4. Identifying the original dataset. This study uses DPC, MODIS, ERA5, HYCOM and AERONET data. However, some descriptions are missing regarding product type, time period (start date and end date), dataset size (number of pixels and number of AERONET sites). Please detail as much as possible, and if not sufficient, use Appendix to describe the data so that readers can collect necessary data.

Thanks for the suggestion. The temporal coverage of this study is primarily constrained by the availability of DPC observations. Specifically, we have six months of DPC data, encompassing April, July, and October 2019, as well as January–March 2020. The MODIS,

ERA5, HYCOM, and AERONET teams provide continuous data covering this period, enabling the retrieval and validation in this study. We have added this information in the manuscript in L75-77:

> *Six months of DPC Level 1 data, encompassing April, July, and October 2019, as well as January-March 2020, are used in the retrieval in this study. The AERONET, MODIS, as well as other auxiliary data are selected from the same periods.*

The temporal and spatial resolution of the auxiliary data are described in Sect. 2.2 in the manuscript. We have summarized them in Table 1 in the manuscript.

5. Describing applied corrections and filters. It appears that authors have applied some corrections to DPC data, but the details are not presented. Some references are provided, but it would be beneficial to briefly describe the outline of the applied corrections. In addition, the "fine-mode filtering" of AERONET data (and potentially retrieval results) remains unclear. Documenting the number of points (pixels) before and after filtering would help readers understand the extent of filtering.

Thanks for the suggestion. Following the launch of DPC, gradual aging of its optical components led to a drift in radiometric response, with the magnitude of the drift related to both time and VZA. Zhu et al. (2022) calibrated this drift using DPC observations over deep ocean regions through the Rayleigh method and provided monthly VZA-dependent calibration coefficients. In this study, DPC observations were corrected using these calibration coefficients to reduce radiometric biases as much as possible. We have added details about the calibration in the manuscript in L82-89:

> *The radiometric response of DPC/GaoFen-5 is progressively drifting over time and is realted to VZA. Zhu et al. (2022) developed a method based on Rayleigh scattering over the ocean to correct this drift. In deep ocean regions with very low aerosol loading and low surface reflectance, the TOA radiance observed by satellite sensors is dominated by atmospheric Rayleigh scattering, which can be accurately simulated using radiative transfer models. By comparing simulated radiances with DPC observations over such regions, Zhu et al. (2022) provided*

monthly VZA-dependent calibration coefficients at 443, 490, 565, and 670 nm. The calibration uncertainties are about 1-7 % (depending on the wavelength and VZA). In this study, these Rayleigh scattering-based calibration coefficients are applied to correct DPC's scalar reflectance at 443, 490, 565, and 670 nm.

In this study, only the official AERONET Level 2.0 quality control criteria (excluding the AOD threshold) were applied to the Level 1.5 inversion data to ensure the accuracy of AERONET SSA. No additional screening was applied to AERONET observations. However, quality control was performed on the retrieval results, based on whether the retrieved parameters exceeded predefined thresholds. Retrievals yielding physically unreasonable values outside these thresholds were regarded as failed cases and were excluded from further analysis. The predefined thresholds have been summarized in Table 3 in the manuscript.

6. Clarifying the measurement vector, a priori state vector, model parameters, and variance-covariance matrix in the retrieval algorithm. The developed algorithm is based on optimal estimation. Optimal estimation is a blending of measurements and a priori information based on variance, and therefore the information on the a priori state vector, model parameters, and variance-covariance matrices should be documented and the reasons behind the choice should be described. This shortcoming makes the study non-reproducible and the interpretation of results very challenging. In addition, the measurement vector elements remain ambiguous. It is requested to document the used spectral channel, polarization or not, and the filtering applied to the input data.

Thanks for this important suggestion. We agree that a clear and complete description of the measurement vector, the a priori state vector, the model parameters, and the associated variance-covariance matrices is essential. In the revised manuscript, we have expanded the description of the retrieval algorithm, and added two tables (Tables 2 and 3) to summarize these settings. Specifically, Table 2 summarizes the selected DPC measurements and their associated uncertainty specifications, while Table 3 lists the prescribed a priori values and uncertainties for aerosol and surface parameters.

In particular, we have clarified the composition of the measurement vector **y**, including the spectral channels, the use of polarization information, and the angular sampling strategy, in L167-173:

> *The measurement vector, $\boldsymbol{y}$, is constructed with calibrated scalar reflectance at 443, 490, 565, and 670, as well as DOLP at 490 and 670 nm from several angles…Pixels with fewer than 9 viewing angles, which are primarily located near the scan edges, were therefore excluded. For the remaining pixels, observations from the first 9 viewing angles were used in the retrieval to maintain a fixed number of viewing angles for all pixels.*

The measurement error covariance matrix is calculated based on DPC calibration uncertainties, which has also been specified in L176-178:

> *Therefore, this study adopts the official pre-launch laboratory calibration errors, namely 5 % radiance errors and 0.02 DOLP errors (Li et al., 2018), as the observational errors used to construct the measurement error covariance matrix.*

In addition, the retrieval parameters composing the state vector **x** and the model parameterization used over land and water have been made explicit in L180-189:

> *The state vector, $\boldsymbol{x}$, is composed of aerosol and surface parameters. Particularly, for land surfaces, the state vector $\boldsymbol{x}$ consists of AOD ($\tau(\lambda)$), SSA ($\omega(\lambda)$), kernel intensity parameters of RTLS model ($K(\lambda)$, k_{vol}, and k_{geo} in Eq. 2), and the scale factor of BPDF-NDVI model (C in Eq. 8)…For water surfaces, only $\tau(\lambda)$ and $\omega(\lambda)$ are retrieved as components of the state vector $\boldsymbol{x}$, and the New Cox-Munk model is implemented to compute the surface reflectance (Spurr, 2006). The wavelength-dependent parameters, $\tau(\lambda)$, $\omega(\lambda)$, and $K(\lambda)$, are retrieved at 443, 490, 565, and 670 nm, corresponding to the wavelengths at which DPC observations are used to construct the measurement vector.*

The description of a priori values and the corresponding uncertainties has been clarified in L189-192:

For AOD and SSA, the a priori state vector and its associated error covariance matrix are prescribed as fixed values, derived from the mean and variance of AERONET measurements. The a priori estimates of surface properties are also fixed, with their errors defined by the corresponding ranges of variability.

Finally, we have stated that the cost function minimization is implemented through an iterative Gauss–Newton approach (L201):

The algorithm minimizes the cost function defined in Eq. 4 using an iterative Gauss–Newton method to obtain the final retrieval results.

We believe these revisions address the reviewer's concerns by documenting the measurement vector elements, the state vector and model parameterization, and the variance-covariance assumptions and a priori settings, with configurations listed in Tables 2 and 3.

7. Improving the compatibility with other studies. The validation sections discuss mainly the results at 443 nm, but a number of previous research use 550 nm for comparison. The contribution of fine-mode particles is substantially different between two wavelengths and presented results are not directly comparable. Even if the results at 550 nm may not be very encouraging, it serves the community to understand what to improve in the next instrument and algorithm development.

Thanks for the suggestion. The retrieval results of this study are primarily validated against AERONET observations, which provide high-quality aerosol measurements and are widely used as a reference dataset. Particularly, AERONET inversion products are available at 440, 675, 870, and 1020 nm, thus an important consideration for focusing on the 440 nm results is the direct availability of AERONET observations at this wavelength. In the revised manuscript, we have added results at additional wavelengths and included comparisons with other studies.

Other satellite products, such as the widely used MODIS AOD, mainly provide retrievals at 550 nm and are commonly applied in large-scale or spatial pattern analysis. Accordingly,

maps of the retrieval results at 550 nm have been included in the Supplement and compared with MODIS AOD.

7. Deepening the analysis of the case study and global statistics. Although authors mention in the conclusions that the analysis remains qualitative, there are unexplained patterns and characteristics in the case study and the global map. Figure 9 seems to be influenced by the number of view directions (bands-like patterns running in satellite cross-track direction) and Figures 10 and 11 show the difficulties probably related to cloud mask (Southern Ocean AOT values) and view geometry (sharp contrast of SSA that stretches along the orbit).

We thank the reviewer for the helpful comment.

(5) In this study, the number of viewing angles used in the retrieval are fixed. We screened pixels with fewer than 9 viewing angles, and only use observations from the first 9 viewing angles for the remaining pixels. We have added this detail in the manuscript in L171-173:

Pixels with fewer than 9 viewing angles, which are primarily located near the scan edges, were therefore excluded. For the remaining pixels, observations from the first 9 viewing angles were used in the retrieval to maintain a fixed number of viewing angles for all pixels.

Therefore, the band-like patterns in Figure 9 are probably not caused by the number multi-angle observation itself. Instead, they might be related to variations in viewing-angle distribution between successive cross-track scans of DPC.

As mentioned in the revised manuscript in L79:

However, after launch, DPC exhibited a gradual change in radiometric sensitivity, primarily due to aging of the optical components. This drift is dependent on both wavelength and field of view and can introduce increasing systematic biases if not properly corrected.

Due to aging of the DPC optical components, the radiometric response experienced VZA-dependent drift. When the satellite switches from one cross-track scan to the next, the

distribution of viewing angles changes sharply. As a result, the magnitude of radiometric drift may differ between adjacent scans. Although radiometric calibration is applied before the retrieval process, this correction cannot completely remove the VZA-dependent residual errors. These residual differences may lead to meridional discontinuities in the retrieval results.

We have revised the manuscript in L389-396 to clarify this explanation:

> *The meridional discontinuities in Fig. 9(b,c) primarily originate from abrupt changes in the observed radiance between successive cross-track scans of DPC, rather than from the retrieval algorithm itself. These discontinuities arise when the instrument switches from one cross-track scan to the next, during which the distribution of viewing angle changes. Due to aging of the DPC optical components, the radiometric response exhibits VZA-dependent drifts. Consequently, variations in viewing-angle distribution lead to variations in the magnitude of this drift, leading to radiance inconsistencies between adjacent scans. Although radiometric calibration is applied prior to the retrieval, the VZA-dependent residual errors cannot be completely eliminated. These residual radiometric differences ultimately result in the meridional striping patterns seen in the retrieval results.*

(4) As for the abnormally high AOD values observed over the Southern Ocean in Fig. 10, we conducted further examinations using true-color imagery and MODIS AOD products. The true-color imagery for early January 2020 reveals extensive smoke plumes over the Southern Ocean originating from southeastern Australia and gradually transported eastward. This indicates that large amounts of biomass-burning aerosols were present over the region during this period. The MODIS monthly AOD product for January 2020 also shows anomalously high AOD over the Southern Ocean, with values exceeding 0.5 in some areas (Fig. R3-1). The spatial pattern and magnitude are generally consistent with our retrieval results. Thus, this magnitude is likely reasonable. We have added the corresponding MODIS AOD map to the Supplement material, and included a relevant discussion in the manuscript in L440-442:

The anomalously high AOD over the Southern Ocean in January 2020 reaches values of up to 0.5 in some regions, consistent with independent data sources (e.g., MODIS AOD, see Supplement).

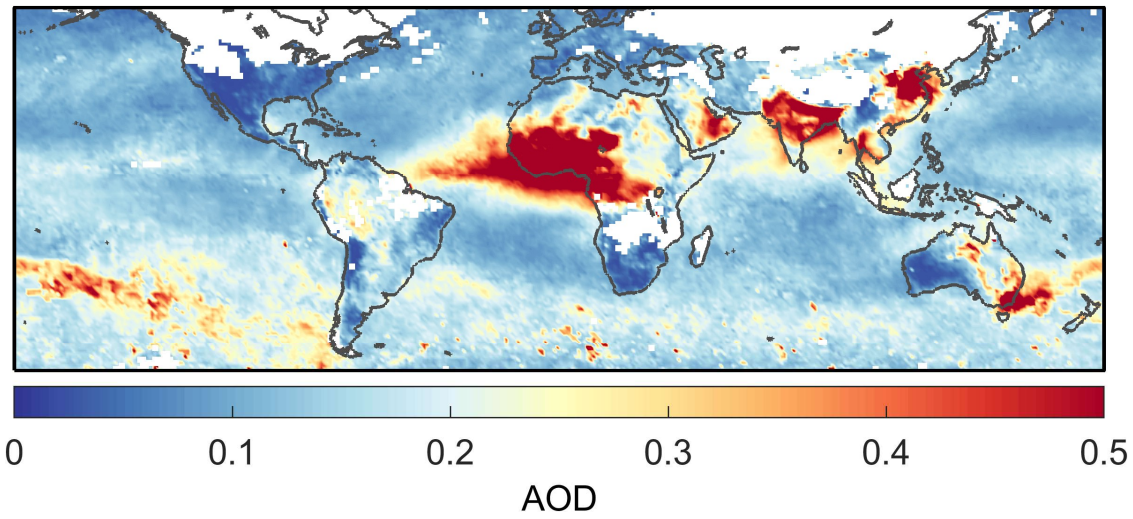

Fig. R3-1. Global AOD for January 2020 at 550 nm from MODIS/Aqua Level 3 product.

(5) We agree that the sharp zonal contrast of SSA along the orbit is closely related to viewing geometry effects. In the revised analysis, we further examined the impact of ocean glint geometry. When the glint angle is small (≤ 40°), enhanced surface reflection over ocean increases the sensitivity of the retrieval to geometry-related biases. After excluding oceanic pixels with glint angle ≤ 40°, the sharp contrast of SSA along the orbit is substantially reduced, and the spatial continuity of the retrievals is significantly improved. This improvement confirms that the previously observed discontinuities are indeed strongly associated with viewing geometry effects. We have updated the global maps, removed the previous statements regarding zonal discontinuities, and added a detailed description of the pixel-screening procedure in the revised manuscript in L198:

Pixels with glint angle ≤ 40° over ocean are also excluded, because enhanced specular reflection at small glint angles reduces the aerosol information content and may introduce geometry-dependent artifacts.

Specific comments:

5. Line 44: It is somewhat misleading to claim that DPC follows up the data gap after the retirement of the POLDER sensors because there are no Chinese investments in international public data dissemination to my knowledge. If there is any news about this, please comment or refer to an article. This is important for the European community that is the main target of this journal.

Thanks for reminding. We have revised the expression in the manuscript in L41:

After the retirement of POLDER in 2013, operational spaceborne multi-angle polarimetric observations became limited. The launch of the Directional Polarimetric Camera (DPC) onboard Gaofen-5 in 2018 introduced a new source of multi-angle polarimetric measurements. These observations have supported developments in SSA retrievals in recent years.

6. Line 76: "theoretical correction errors". This expression is confusing. Is this the magnitude of correction, or the remaining bias after applying the correction? Please clarify.

We are sorry for the confusion. What we intend to convey is that this uncertainty originates from the calibration method itself, which are related to uncertainties of input parameters. We have revised the expression in the manuscript in L87:

The uncertainty associated with the calibration method is about 1-7 % (depending on the wavelength and VZA).

7. Lines 84-86: "Considering relatively …". Two referenced papers are not providing the ground to use a single aerosol model to analyze polarimetric measurements. Both studies focused on MODIS retrievals.

We are sorry for the confusion. We agree that the two cited studies focused on MODIS scalar retrievals and therefore do not directly justify the use of a single aerosol model for polarimetric measurements. In both studies, sensitivity experiments were conducted by employing different aerosol models, and the results indicated that retrieval errors induced by the phase matrix were smaller than those associated with AOD, SSA, and surface albedo.

However, these analyses were based on single-angle scalar observations rather than polarization measurements. To address this concern more rigorously in the present study, we have added additional sensitivity experiments to explicitly evaluate the impact of the aerosol phase matrix within our retrieval framework. The results confirm that, although some variability is introduced by different phase matrices, the induced uncertainties remain smaller than those associated with other parameters. The corresponding analyses and discussions have been incorporated into the revised manuscript in Sect. 3.1 to provide a more solid justification for the adopted aerosol model configuration.

8. Lines 121-122: "accurately", "high-precision". The relevance to this paper is the accuracy and precision needed for this research. Unless there are strict requirements that limits the choice of radiative transfer models, I suggest removing these non-quantitative expressions.

We thank the reviewer for the suggestion. We agree that the terms "accurately" and "high-precision" are qualitative and not strictly quantified in this context. Since this study does not impose explicit accuracy or precision constraints that would limit the choice of radiative transfer models, these expressions have been removed to avoid overstatement. We have revised the expression in L135-137 to focus on the functional capabilities of the model rather than qualitative performance descriptions:

> *It simulates Stokes vectors and their linearized matrices (Jacobians) at arbitrary altitudes and viewing geometries, providing radiative simulations for satellite remote sensing applications and serving as an effective forward model in numerical inversion algorithms (Spurr, 2006).*

8. Line 157: "fixed constants". Optimal estimation is a blending of a priori and measurements, and therefore the assumption used in the a priori can easily bias the estimation when the measurement information content is not sufficient. The precise values used in this study should be presented with reasons of choice.

We thank the reviewer for the insightful comment. We agree that, in general, the choice of a priori assumptions in optimal estimation may influence the retrieval when the measurement information content is limited. In this study, however, the focus is on

evaluating the robustness and reliability of the retrieval algorithm itself under a controlled and simplified configuration. Therefore, fixed a priori values and associated errors are adopted to ensure consistency and reproducibility of the results. The a priori values and associated errors for AOD and SSA are derived from the mean and standard deviation of AERONET observations, providing physically reasonable and observationally based constraints. The a priori estimates of surface properties are also prescribed as fixed values, with their associated uncertainties defined according to the corresponding ranges of variability. These a priori values and associated errors have been documented in Table 3 in the manuscript, and a corresponding description has been added in L189-194:

> *For AOD and SSA, the a priori state vector and its associated error covariance matrix are prescribed as fixed values, derived from the mean and variance of AERONET measurements. The a priori estimates of surface properties are also fixed, with their errors defined by the corresponding ranges of variability. The use of fixed a priori values is intended to provide a controlled and consistent configuration for evaluating the inherent performance of the retrieval algorithm. Details of the a priori values and associated errors are summarized in Table 3.*

8. Line 211: This section presents the results of numerical simulation, but the simulation geometry is not mentioned anywhere, limiting the reproducibility of the obtained results.

We thank the reviewer for pointing out this missing description. We agree that a clear description of the simulation geometry is essential for the reproducibility of the sensitivity experiments. In the revised manuscript, we have listed the SZA, VZA, and RAA in Table 4 used in the simulations. We have also added details in the manuscript in L216:

> *The simulations were conducted under a series of SZA, VZA, and RAA, as listed in Table 4.*

8. Lines 215-216: “not sensitive”. This sentence is an overstatement as only one aerosol model and two land surface models are employed. It also contradicts to the previous studies, notably to the study of critical surface albedo by Seidel and Popp (2012).

We thank the reviewer for this important comment. We agree that the term "not sensitive" was inappropriate and could be misleading in this context. The intended meaning of the original statement was not that the magnitude of the response is insensitive to surface parameters, but rather that, for the two land surface models considered, the response patterns of ΔI and ΔDOLP to prescribed SSA perturbations are similar. We have revised the text accordingly to emphasize the similarity in the overall trends, while explicitly acknowledging the presence of differences in magnitude and angular distribution. We have revised the expression in the manuscript in L253-255:

> *Despite minor differences in magnitude and angular distribution, the changes in I and DOLP induced by the prescribed SSA perturbations exhibit similar overall patterns for the two land surface models considered.*

The revised expression avoids overgeneralization and does not imply a general insensitivity to surface properties.

9. Figure 2, 3, and 4: Fluctuating results from the radiative transfer simulation of such smooth phase function is surprising. Are small fluctuations of these curves significant? What is the precision of the radiative transfer simulation in this study? Adding error bound and explanation in the main text deems necessary.

Thank you for this constructive comment. The scattering angle is calculated from various combinations of SZA, VZA, and RAA, which are grouped into bins and are now listed in Table 4 in the revised manuscript. For similar scattering angles, the corresponding SZA-VZA-RAA combinations may differ substantially. Such differences may lead to distinct atmospheric photon path lengths in the radiative transfer calculations. In addition, the surface reflectance is also anisotropic, which may also attribute to variations in simulated TOA radiance. To further clarify this issue, we have provided the error bounds in the updated figures. The error bounds are now explicitly reported in the manuscript.

9. Line 251: In this section (Section 3.2) and in the following section (Section 3.3), I consider that it is necessary to perform the performance comparison at 550 nm (or 565 nm) rather than at 443 nm. Otherwise, this manuscript is not comparable to other previous publications that authors themselves referenced. As authors mention

near Line 285, the retrieval performance depends on wavelength and available information. This is why the comparison at an inconsistent wavelength is not adequate.

We thank the reviewer for this important comment. In the revised manuscript, we have added the corresponding analysis at 565 nm in Sects. 3.2 and 3.3. This ensures better comparability with prior publications and provides a more appropriate evaluation of the retrieval performance across wavelengths.

11. Line 254: "443 nm AOD". This has to be kept as AOT at 443 nm, even when comparing the performance of AOT and SSA at 550 nm, in order to be consistent with AERONET processing algorithm that applies the "fine mode filter" by AOT 440 nm.

We thank the reviewer for pointing it out. We have revised the text to explicitly state that the fine-mode filtering is consistently based on AOD at 443 nm, in line with the AERONET processing algorithm that applies the filter at 440 nm. This AOD (443 nm) threshold is used solely as a selection criterion for SSA validation and is applied uniformly throughout the analysis, independent of the wavelength at which AOD or SSA performance is evaluated. The expression in the manuscript has been revised in L295-298:

For this reason, the validation applied an AOD-based screening criterion using AOD_{443} (AOD at 443 nm). Only SSA retrievals with $AOD_{443} > 0.4$ were retained, consistent with the AERONET fine-mode filtering criterion. This criterion was applied uniformly throughout the analysis, independent of the wavelength at which AOD or SSA was evaluated.

12. Line 288: Same comment as Line 251 for this section.

Thanks for the comment. As mentioned above, analysis at 565 nm has also been added in Sect. 3.3.

13. Line 292: "similar performance". This reads contradictory to Line 266, "relatively weaker performance". The correlation coefficient of SSA drops from 0.688 at 443

nm to 0.347 at 565 nm, and it is difficult to claim that the performance at 565 nm is "similar" to that at 443 nm.

We are sorry for the confusion. We agree that the phrase "similar performance" was inappropriate and could be misleading, given the clear degradation in SSA retrieval performance from 443 nm to 565 nm. The intended meaning was that the wavelength dependence of the retrieval performance, namely the decreasing performance with increasing wavelength, is consistent with the behavior observed in the simulated-data experiments. However, in the revised manuscript, we have updated the retrieval experiment, and the expression about "similar performance" has been removed.

14. Line 299: "comparable to the operational MODIS AOD product (Levy et al., 2010)". This claim is an overstatement. The referenced paper reports the correlation coefficient of 0.896 for AOT at 470 nm and 0.882 for AOT at 550 nm. This sentence claims that correlation coefficient of 0.75 for AOT at 443 nm is comparable.

We thank the reviewer for this comment. We agree that the correlation coefficient of 0.75 obtained in this study is lower than those reported for the operational MODIS AOD product in Levy et al. (2010), and the original expression was therefore an overstatement. The text has been revised in L334-336 to acknowledge that the performance is weaker than that of the operational MODIS product, while still indicating that the retrieved AOD shows a reasonable level of consistency with AERONET observations:

This performance is slightly lower than that reported for the operational MODIS AOD products (Levy et al., 2010), but it is comparable in terms of AOD correlation to the DPC retrievals reported by Dong et al. (2024), who obtained a correlation coefficient of 0.76 for AOD at 670 nm.

15. Line 339: "strong absorption properties". In Levy et al. 2007a, heavy smoke by biomass burning is recommended to be modeled by their "absorbing" model, instead of "moderately absorbing" model, while this study uses their "moderately absorbing" model and employ the heavy smoke case as a case study. It is worth mentioning the reasons behind the inconsistency.

Thank you for this insightful comment. To address this concern, we conducted additional sensitivity experiments in Sect. 3.1 to quantify the impact of using different phase matrices on the retrieval results. We also present the results in Fig. R3-2. The analysis shows that the errors introduced by the choice of phase matrix are relatively small. Therefore, the use of the "moderately absorbing" model does not lead to significant biases in the heavy smoke case considered in this study.

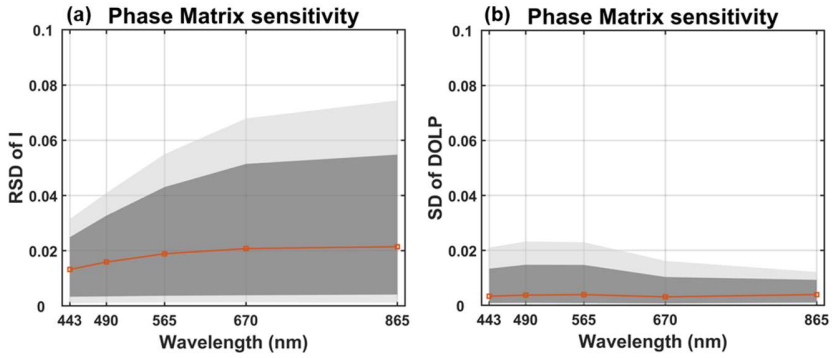

Fig. R3-2. Relative standard deviation (RSD) of I (a) and standard deviation (SD) of DOLP (b) induced by variations in phase matrix.

Technical comments:

6. Line 67: "normalized radiation". normalized radiance

Thanks for reminding. We have revised the expression in the manuscript.

7. Lines 140-141, 145: xa. Using xa as a-posteriori state vector is rather confusing as Sa is used for a-priori variance-covariance matrix. I suggest replacing by x^ (x-hat, circumflex above x) , following the common convention.

Thanks for the suggestion. We have replaced $\mathbf{x}^{\mathbf{a}}$ with $\hat{\mathbf{x}}$ in the manuscript.

Reference

Dong, Y., Li, J., Zhang, Z., Zheng, Y., Zhang, C., & Li, Z. (2024). Machine learning-based retrieval of aerosol and surface properties over land from the gaofen-5 directional polarimetric camera measurements. *IEEE Transactions on Geoscience and Remote Sensing*, *62*, 1–15. https://doi.org/10.1109/tgrs.2024.3419169

Levy, R. C., Remer, L. A., & Dubovik, O. (2007). Global aerosol optical properties and application to moderate resolution imaging spectroradiometer aerosol retrieval over land. *Journal of Geophysical Research: Atmospheres*, *112*(D13), D13210. https://doi.org/10.1029/2006jd007815

Levy, R. C., Remer, L. A., Kleidman, R. G., Mattoo, S., Ichoku, C., Kahn, R., & Eck, T. F. (2010). Global evaluation of the collection 5 MODIS dark-target aerosol products over land. *Atmospheric Chemistry and Physics*, *10*(21), 10399–10420. https://doi.org/10.5194/acp-10-10399-2010

Li, Z., Hou, W., Hong, J., Zheng, F., Luo, D., Wang, J., et al. (2018). Directional polarimetric camera (DPC): Monitoring aerosol spectral optical properties over land from satellite observation. *Journal of Quantitative Spectroscopy and Radiative Transfer*, *218*, 21–37. https://doi.org/10.1016/j.jqsrt.2018.07.003

Zhu, S., Li, Z., Qie, L., Xu, H., Ge, B., Xie, Y., et al. (2022). In-flight relative radiometric calibration of a wide field of view directional polarimetric camera based on the rayleigh scattering over ocean. *Remote Sensing*, *14*(5), 1211. https://doi.org/10.3390/rs14051211

Report 4

Reply to Anonymous Referee #5

This study develops a numerical inversion algorithm to simultaneously retrieve AOD, SSA, and land surface reflectance using multi-angle polarimetric data from the Gaofen-5 DPC. By employing an optimization-based approach and validating against both simulated data and AERONET observations, the authors demonstrate the potential of DPC for global aerosol monitoring. While the topic is relevant and the retrieval framework shows promise, significant concerns remain regarding the methodology's novelty, the representativeness of the simulated data, and the rigor of the validation process. My specific comments are as follows:

The authors appreciate the reviewer for the constructive comments and thoughtful suggestions, which are very helpful in improving our manuscript. We have carefully considered all the comments and revised the manuscript accordingly. Below is a detailed point-by-point response to these comments.

7. The English expression should be refined to meet academic writing standards.

We thank the reviewer for this comment. We have revised the manuscript and improved the expression.

8. Lines 54-56: please clearly justify what novel contribution this work makes beyond RemoTAP, GRASP, and ML-based approaches.

We thank the reviewer for this important comment. The novelty of this work does not lie in proposing a new inversion theory, but in extending a physically based inversion framework to enable global-scale SSA retrieval from DPC observations, which has not yet been comprehensively demonstrated. While global DPC AOD products already exist, applications of GRASP- or RemoTAP-type methods to DPC-based SSA retrieval have so far been limited to regional studies. In addition, GRASP and RemoTAP typically retrieve aerosol microphysical parameters as intermediate variables, while this study directly retrieves commonly used optical properties (AOD and SSA) within the same physical

inversion framework. This represents an alternative implementation strategy rather than a fundamental methodological difference.

Regarding ML-based approaches, although they have demonstrated strong performance, they rely on representative training datasets, and their performance may decrease in regions or conditions with limited observations. For example, Dong et al. (2024) reported anomalously high AOD values over South America in October 2019, whereas both our results and the MODIS AOD show relatively low values in that region. The physically based framework adopted here does not depend on training samples and is therefore better suited for consistent global-scale applications.

We have also revised the manuscript in L55-59 to clarify these points:

> *Moreover, although machine learning approaches have demonstrated strong performance, they are typically data-driven and rely on the availability of representative training samples, without explicitly modeling the underlying physical mechanisms. As a result, their performance may decrease in regions or conditions with limited observations. On the other hand, studies applying physically based inversion methods to DPC observations for global SSA retrieval are still relatively limited. Further efforts are therefore needed to extend such physically based approaches on the global scale.*

8. Section 2.8: there is no evidence that the simulated data realistically represent actual DPC observations, and the manuscript fails to quantify potential biases arising from the integration of multiple data sources.

Thank you for the comment. In Sect. 2.8, the simulated measurements were designed to be consistent with DPC observations in both geometry and uncertainty. Specifically, we added Gaussian noise to the simulations using the DPC laboratory calibration uncertainties, i.e., an error of 5% scalar reflectance and an error of 0.02 for DOLP. The retrieval experiment using simulated data is motivated by the fact that the actual on-orbit observation errors are difficult to quantify. Therefore, we use a simulated dataset with controlled errors to evaluate retrieval performance under well-defined measurement uncertainties.

The observation geometry used in the simulations (including SZA, VZA, and RAA) was taken from the corresponding DPC measurements, so the angular sampling matches real DPC viewing conditions. The DPC observations were also matched with AERONET aerosol products and MODIS surface data to better reflect actual atmospheric and surface conditions at the time and location of the DPC overpass.

Regarding potential biases from integrating multiple data sources, we emphasize that our retrieval experiment is conducted on simulated observations with controlled measurement errors, and the retrieval results can be compared directly with the known "true" inputs used in the forward simulations. This avoids additional ambiguity from errors in validation data, and provides a clear baseline for diagnosing algorithm performance.

9. Lines 157-159: how the multi-angle information from DPC is utilized in the proposed retrieval method?

We thank the reviewer for this comment. Measurements of scalar reflectance and DOLP from multiple viewing angles are jointly used in the inversion, together constructing the measurement vector. These multi-angle measurements are simultaneously fitted within a unified inversion scheme through a least-squares optimization. The multi-angle observations are particularly important for constraining angular dependence of surface reflectance, which helps reduce the coupling between surface and atmospheric contributions and improves the stability of the retrieval. The usage of multi-angle measurements have been added to the revised manuscript in L167-174:

> *The measurement vector, $\boldsymbol{y}$, is constructed with calibrated scalar reflectance at 443, 490, 565, and 670, as well as DOLP at 490 and 670 nm from several angles… Consequently, the scalar reflectance and DOLP at each wavelength consist of measurements acquired from 9 viewing angles.*

9. Lines 200-202: it is unclear whether the actual DPC observation scattering angle distribution has been considered.

We thank the reviewer for pointing out this missing information. The actual DPC observation geometry was considered in the simulations. The SZA, VZA, and RAA used

in the simulations were taken from the matched DPC observations, thereby accounting for the actual scattering angle distribution of DPC observations. We have added this information in the manuscript in L223-227:

> *The simulated dataset was constructed using aerosol parameters derived from daily AERONET observations selected within an 8 km radius of DPC overpass locations to represent typical aerosol conditions observed by DPC. The corresponding viewing geometry, including SZA, VZA, and RAA, was taken from the matched DPC observations and used in the radiative simulations, thereby accounting for the actual scattering angle distribution of DPC observations.*

9. Section 3.1: the authors should clarify its relevance to the study.

Thank you for this comment. Sect. 3.1 is included to explain the practical difficulty of retrieving SSA from DPC-like measurements. The sensitivity experiment quantifies the changes in I and DOLP induced by small SSA perturbations, and shows that in many situations these changes are comparable to, or smaller than, the current measurement accuracy. This directly helps interpret why SSA retrievals often have relatively large uncertainties in existing products, and it also provides a quantitative reference for the observation accuracy required to improve SSA retrieval performance in future instruments.

9. Figure 5: the same AERONET-MODIS matched dataset both to generate the simulated observations and to validate the retrievals? Please clearly clarify this point.

We are sorry for the confusion. The AERONET-MODIS matched dataset is used as the reference atmospheric and surface parameters (refered as the "true values" in the manuscript) to simulate the TOA radiance that would be received by the DPC instrument through a forward radiative transfer model. These simulated radiances are then taken as input to the retrieval algorithm, and the retrieved results are finally compared with the same reference dataset ("true values") to evaluate the retrieval performance. Therefore, the matched AERONET-MODIS dataset serves as the physical "truth" for a controlled retrieval experiment, which is a common approach to assess algorithmic performance under idealized conditions.

10. Figure 7: The validation accuracy against AERONET is markedly lower than that obtained with simulated data; how do the authors justify the reliability of the simulation-based validation? Are the AERONET datasets used for simulation-based and real-observation validation independent, or is there potential overlap that could bias the results?

We thank the reviewer for this comment. The higher accuracy in the simulation-based validation is expected and does not imply that the same performance can be achieved for real DPC observations. The simulation experiment is a controlled retrieval test (the construction workflow of simulated dataset has been clarified in our response to the previous comment and in the revised manuscript), and its better performance mainly comes from: (1) controllable observation errors in the simulated TOA radiances, whereas real DPC measurements may have larger uncertainties which have not yet been well quantified (e.g., DPC DOLP uncertainty may exceed 0.04; scalar reflectance calibration reduces systematic biases but random errors remain); (2) comparison against a prescribed "truth" without additional measurement uncertainty, while real-observation validation against AERONET inevitably includes uncertainty in the reference itself (e.g., AERONET SSA uncertainty is ~0.03); and (3) a more consistent forward-inverse modeling setting, which reduces model-mismatch effects compared with real observations (this factor is likely secondary). We have revised the manuscript in Sect. 3.3 to state these points more clearly, and to avoid potential misunderstanding about the relationship between the simulation-based evaluation and the real-observation validation:

10. Lines 318-320: this explanation is not convincing, as such pronounced striping is not evident in the corresponding true-color imagery.

We thank the reviewer for this helpful comment. The true-color image used for comparison is from MODIS and VIIRS, which provide single-view scalar observations with smoothly varying viewing geometry. In contrast, DPC uses multi-angle polarimetric measurements, and viewing-angle discontinuities can occur between adjacent scans. When the satellite switches from one cross-track scan to the next, the distribution of viewing angles changes sharply. Moreover, due to aging of the DPC optical components, the radiometric response experienced VZA-dependent drift. Therefore, the magnitude of radiometric drift may differ

between adjacent scans. Although radiometric calibration is applied before the retrieval process, this correction cannot completely remove the VZA-dependent residual errors. These residual differences may lead to meridional discontinuities in the retrieval results.

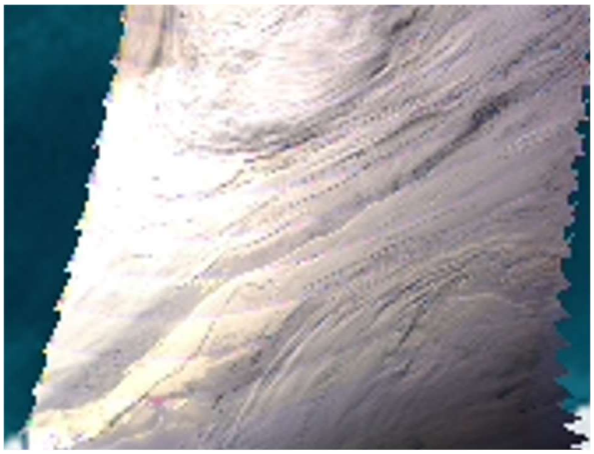

Fig. R4-1. An example of true-color image from DPC observation.

We further examined DPC true-color imagery for verification. Because the resolution of DPC true-color imagery is lower, and over bright desert surfaces the striping is less visible due to limited contrast. In comparison, over more uniform backgrounds with better contrast, such as vegetated areas or scenes dominated by optically thick clouds, the striping pattern is much easier to identify.

We have revised the manuscript and added a more detailed discussion in L389-396:

> *The meridional discontinuities in Fig. 9(b,c) primarily originate from abrupt changes in the observed radiance between successive cross-track scans of DPC, rather than from the retrieval algorithm itself. These discontinuities arise when the instrument switches from one cross-track scan to the next, during which the distribution of viewing angle changes. Due to aging of the DPC optical components, the radiometric response exhibits VZA-dependent drifts. Consequently, variations in viewing-angle distribution lead to variations in the magnitude of this drift, leading to radiance inconsistencies between adjacent scans. Although radiometric calibration is applied prior to the retrieval, the VZA-dependent residual errors*

cannot be completely eliminated. These residual radiometric differences ultimately result in the meridional striping patterns seen in the retrieval results.

12. Figure 10: The cloud masking appears to be problematic, resulting in extensive missing retrievals and apparent errors in the global 440 nm AOD product.

We thank the reviewer for this important comment. We agree that the cloud screening in the previous version was not sufficiently robust in some regions. We found that some abnormal retrievals are mainly caused by residual cloud contamination, such as the anomalously high AOD at high latitudes in Fig. 10(c,d), and the abnormally low SSA values over South America in Fig. 11(b) and over northern Asia in Fig. 11(c). The extensive areas with missing retrievals are primarily due to persistent cloud cover in that month, and partly to the removal of otherwise clear pixels during cloud masking.

In the revised manuscript, we have implemented a more rigorous cloud screening procedure to mitigate these issues. To reduce the risk of retaining cloudy pixels, we adopted more conservative thresholds. For example, given that the uncertainty at 865 nm can be as large as ~23%, we increased the screening threshold by 20%. Over land, the criterion (R_{865}/R_{443}) was adjusted from 1.2 to 1.44. Over ocean, the threshold was adjusted from 0.40 to 0.32. This tightening is intended to maintain robust cloud removal even when the uncalibrated 865 nm reflectance is positively biased. Following this update, the artifacts mentioned above are substantially reduced, and the global patterns exhibit improved spatial consistency. Nevertheless, the stricter screening inevitably excludes more valid clear-sky pixels, resulting in reduced spatial coverage. It is difficult to simultaneously maintain broad data coverage and completely eliminate cloud contamination. In the revised version, greater emphasis is placed on more rigorous cloud screening to ensure reliable retrieval results, which inevitably leads to reduced spatial coverage.

Reference

Dong, Y., Li, J., Zhang, Z., Zheng, Y., Zhang, C., & Li, Z. (2024). Machine learning-based retrieval of aerosol and surface properties over land from the gaofen-5 directional

polarimetric camera measurements. *IEEE Transactions on Geoscience and Remote Sensing*, *62*, 1–15. https://doi.org/10.1109/tgrs.2024.3419169

Zheng, F., Hou, W., & Li, Z. (2019). Optimal estimation retrieval for directional polarimetric camera onboard chinese gaofen-5 satellite: An analysis on multi-angle dependence and a posteriori error. *Acta Physica Sinica*, *68*(4), 040701. https://doi.org/10.7498/aps.68.20181682

Report 5

Reply to Anonymous Referee #2

We thank the reviewer for the constructive comments and thoughtful suggestions, which are very helpful in improving our manuscript. We have carefully addressed all concerns and revised the manuscript accordingly. A point-by-point response is presented below.

General comments

This study focuses on digging the potential of space-borne multi-angular polarimetric sensors to simultaneously retrieve wavelength-dependent optical properties of atmospheric aerosols and the Earth surface, namely the aerosol optical depth (AOD), single scattering albedo (SSA) and directional hemispherical reflectance (DHR). The sensitivity study highlights sensitivities of multi-angle intensity and polarimetric measurements to SSA at different wavelengths and under different AOD loadings, leading to the demand of an accuracy better than 5% for intensity and 0.01 for DOLP measurements, respectively to retrieve SSA with 0.03 uncertainty. The study can contribute to the community by providing aerosol and surface properties retrieved from DPC data, while I have some major concerns related to the motivation, method, and validation of the study:

1. The motivations of this study are not well demonstrated. The potential and limitations of multi-angular polarimetric observations for aerosol and surface property retrievals has already been well demonstrated by numbers of previous studies, for both POLDER and DPC measurements. The concept of the retrieval method (optimal estimation) has been well established and the retrieval accuracies of AOD, SSA and DHR don't show significant improvement compared with existing algorithms, such as GRASP/PARASOL (Dubovik et al., AMT, 2011; Chen et al., ESSD, 2020) and machine learning methods (Dong et al., TGRS, 2024). Thus, the necessity of developing the retrieval algorithm is not convincing enough. While the motivation of efficiently processing DPC data to generate global aerosol and surface products may stand, it is somewhat regrettable that the retrieval performance over the ocean is not strictly validated in this work.

We sincerely thank the reviewer for the constructive and insightful comments. We appreciate the opportunity to further clarify the motivation and contribution of this study.

We fully agree that multi-angular polarimetric observations have demonstrated strong capability for aerosol and surface property retrievals, and that optimal estimation is a well-established inversion framework. We also acknowledge that the existing algorithms such as GRASP (Chen et al., 2020; Dubovik et al., 2011) and RemoTAP (Hasekamp et al., 2011, 2024) have shown excellent performance in aerosol retrievals. The current limitation mainly concerns SSA retrieval from DPC observations. Existing applications of GRASP- or RemoTAP-type algorithms for DPC-based SSA retrieval have primarily been conducted at regional scales. To our knowledge, global-scale SSA retrievals based on DPC measurements using these numerical inversion frameworks have not yet been reported. One of the main motivations of this study is therefore to generate global aerosol optical products, particularly SSA, from DPC observations within a physically based inversion framework.

Regarding machine learning (ML) approaches, we agree that recent methods have demonstrated competitive performance (Dong et al., 2024). However, their robustness is inherently influenced by the representativeness of the training dataset. In regions with sparse AERONET coverage, the capability of ML-based retrievals may be limited (e.g., the anomalously high AOD values over South America in October 2019 reported by Dong et al. (2024)). A physically based inversion framework provides an independent and potentially more transferable solution for global applications.

Concerning validation over ocean regions, we agree that comprehensive validation is important. However, AERONET-based validation over ocean is limited for several reasons. First, aerosol optical depth over ocean is often relatively low, which makes SSA retrieval from AERONET observations more uncertain and reduces the number of reliable SSA records. Second, the spatial distribution of AERONET sites over oceanic and coastal regions is sparse. Third, the DPC dataset available for this study covers only six months, which further limits the number of collocated samples and prevents large-scale statistical validation. To partially address these limitations, we have added comparisons between our retrieval results and MODIS aerosol products over ocean regions in the revised manuscript.

Although such inter-comparisons cannot fully substitute for AERONET-based validation, they provide useful consistency assessments at broader spatial scales.

2. The retrieval algorithm is not clearly illustrated. The retrieval algorithm is based on the optimal estimation which is a well-established inversion concept, while many aspects are still ambiguous: what are the exact definitions of the utilized measurements and the parameters to retrieve? Are all the spectral, angular, intensity and polarimetric measurements from DPC used? How are the a priori values and covariance matrix determined? How is the optimization procedure realised (iteration step, convergent criteria, initial points, etc.)?

Thank you for this comment. We agree that the retrieval algorithm should be described more clearly within the optimal estimation framework. In the revised manuscript, we have added explicit definitions of both the measurement vector and the state vector, clarified which spectral, polarimetric, and angular DPC observations are used, and explained how the measurement errors and a priori constraints are prescribed. We have also added two tables (Tables 2 and 3) in the manuscript to summarize these information. Table 2 summarizes the usage of DPC measurements and their corresponding error specifications, and Table 3 summarizes the prescribed a priori values and associated uncertainties for aerosol and surface parameters.

In particular, we have clarified that the measurement vector $\mathbf{y}$ is constructed from calibrated scalar reflectance at 443, 490, 565, and 670 nm together with DOLP at 490 and 670 nm, collected from multiple viewing angles (L167-168):

> *The measurement vector, $\boldsymbol{y}$, is constructed with calibrated scalar reflectance at 443, 490, 565, and 670, as well as DOLP at 490 and 670 nm from several angles.*

Since the number of available viewing angles varies among pixels, we have further clarified the angular treatment by excluding pixels with fewer than 9 angles and using a fixed set of 9 viewing angles for all remaining pixels (L171-173):

> *Pixels with fewer than 9 viewing angles, which are primarily located near the scan edges, were therefore excluded. For the remaining pixels, observations from the*

first 9 viewing angles were used in the retrieval to maintain a fixed number of viewing angles for all pixels.

We have also specified that the measurement error covariance matrix is determined based on the official pre-launch calibration uncertainties (L175-178):

Although previous studies have suggested that observational errors of DPC increased after launch (Qie et al., 2021; Zhu et al., 2022), the magnitude of this increase has not been quantitatively characterized. Therefore, this study adopts the official pre-launch laboratory calibration errors, namely 5 % radiance errors and 0.02 DOLP errors (Li et al., 2018), as the observational errors used to construct the measurement error covariance matrix.

In addition, the definition of the state vector $\mathbf{x}$ and the retrieved parameters have been made explicit in L180-189:

The state vector, $\boldsymbol{x}$, is composed of aerosol and surface parameters. Particularly, for land surfaces, the state vector $\boldsymbol{x}$ consists of AOD ($\tau(\lambda)$), SSA ($\omega(\lambda)$), kernel intensity parameters of RTLS model ($K(\lambda)$, k_{vol}, and k_{geo} in Eq. 2), and the scale factor of BPDF-NDVI model (C in Eq. 8)…For water surfaces, only $\tau(\lambda)$ and $\omega(\lambda)$ are retrieved as components of the state vector $\boldsymbol{x}$, and the New Cox-Munk model is implemented to compute the surface reflectance (Spurr, 2006). The wavelength-dependent parameters, $\tau(\lambda)$, $\omega(\lambda)$, and $K(\lambda)$, are retrieved at 443, 490, 565, and 670 nm, corresponding to the wavelengths at which DPC observations are used to construct the measurement vector.

The description of a priori values and their error covariance matrices has been clarified in L189-192:

For AOD and SSA, the a priori state vector and its associated error covariance matrix are prescribed as fixed values, derived from the mean and variance of AERONET measurements. The a priori estimates of surface properties are also fixed, with their errors defined by the corresponding ranges of variability.

Finally, we have stated that the cost function minimization is implemented through an iterative Gauss–Newton approach (L201-202):

> *The algorithm minimizes the cost function defined in Eq. 4 using an iterative Gauss–Newton method to obtain the final retrieval results.*

We believe these revisions resolve the ambiguities noted by the reviewer and provide a clearer and more reproducible description of the retrieval algorithm, including the measurements utilized, parameters retrieved, error characterization, a priori constraints, and optimization strategy.

3. The analysis of the algorithmic accuracy and comparison with other studies are not adequate neither based on simulated data nor based on real measurements. The retrieval from simulated data assumes absolutely accurate measurements fully represented by the radiative transfer model, while it does not assess the influence of measurement noise on the retrieval results. There is also lack of comparison with other multi-angle polarimetric inversion algorithms based on simulated data (e.g., the work by Dubovik et al., (AMT, 2011)) to evaluate the advantages and disadvantages of the retrieval algorithm proposed in this work. Furthermore, when applying to real DPC measurements, there is only a small part (L312-313) mentioning the comparability of SSA correlation coefficient with one study based on DPC data (Fang et al., RS, 2022). If the development of DPC retrieval products is one of the main motivations of this study, more comprehensive comparison of the DPC retrieval accuracy with others studies, such as those you mentioned in Introduction (L47-54), is probably necessary.

Thank you for this detailed comment. We have revised the manuscript to strengthen the evaluation of retrieval accuracy for both simulated and real DPC data, and to add more comparisons with existing studies. For the simulated-data evaluation, we perform retrievals for two simulation settings generated with the same forward model and geometry: a noise-free dataset and a dataset with Gaussian noise added representing the DPC laboratory calibration uncertainties (5% error in I and 0.02 error in DOLP). By comparing the two retrieval results against the known “true” inputs, we explicitly quantify how measurement

noise affects the retrieved parameters, rather than assuming perfectly accurate observations. Particularly, after adding noise, the SSA retrieval performance degrades rapidly: the correlation coefficient decreases from above 0.6 (noise-free case) to below 0.4 (noisy case), indicating that SSA is highly sensitive to measurement uncertainty. We also examined the simulated-data results reported by Dubovik et al. (2011), but their results are presented in a substantially different form and under different evaluation settings, which makes a direct, metric-by-metric comparison difficult.

For the application to real DPC measurements, we note that reported SSA retrieval results from DPC/Gaofen-5 remain limited. In addition to Fang et al. (2022), we added a comparison with the SSA results reported by Dong et al. (2024). The SSA retrievals reported by Jin et al. (2024) mentioned in the Introduction are based on DPC-2/ GaoFen-5(02) measurements, which differ from the instrument configuration used here and cover a different time period, which have been clarified in the revised manuscript. We also acknowledge that discrepancies across studies may arise from differences in calibration and error assumptions, screening, collocation, surface constraints, and aerosol model settings.

Overall, these revisions aim to provide a clearer and more quantitative assessment of algorithmic accuracy, the role of measurement noise, and the relative performance of our approach compared with existing studies.

According to these concerns, more adequate illustration of the motivation and a more comprehensive discussion section might be needed in order to be qualified in the publication in AMT. In addition, there are several statements not true or at least not rigorous enough in the main text. Please see the following comments for more details.

Specific comments

1. L54-56: What do you mean by “lack physical interpretability”? A method is considered as effective as long as its accuracy is sufficiently validated, isn’t it?

Thank you for this comment. We agree that a method can be considered effective if its accuracy is sufficiently validated. In this context, our intention was not to question the effectiveness of machine learning approaches, but to highlight some commonly discussed characteristics of data-driven methods. Many machine learning approaches rely primarily on training data and do not explicitly represent the underlying physical mechanisms. As a result, their performance may depend on the availability and representativeness of training samples, and may degrade in regions or conditions where training data are limited. For example, Dong et al. (2024) used AERONET observations as training samples, which may limit the performance in regions with sparse ground-based measurements (e.g., the anomalously high AOD values over South America in October 2019).

We have revised the manuscript to clarify this point and to avoid overstating the limitation of machine learning approaches:

> *Although machine learning approaches have demonstrated strong performance, they are typically data-driven and rely on the availability of representative training samples, without explicitly modeling the underlying physical mechanisms. As a result, their performance may decrease in regions or conditions with limited observations.*

2. L57-58: It is recommended to insert a short paragraph at the end of the Introduction to briefly describe the structure of the manuscript as well as the main contents of each section.

We thank the reviewer for this helpful suggestion. We have added a short paragraph at the end of the Introduction to outline the structure of the manuscript and to briefly summarize the main content of each section.

> *The remainder of this paper is organized as follows. Sect. 2 describes the data, methods, and experiments conducted in this study. Sect. 3 presents the main results, including sensitivity experiments, validation using simulated data and DPC observations, and regional and global maps of the retrieved parameters. Sect. 4 discusses the results and concludes the paper.*

3. L84-87: The phase matrix is an important microphysical property which depends on aerosol size, shape and refractive index, and which in turn influences aerosol SSA which is the core retrieval parameter throughout this study. Thus, rather than simply referring to other studies, you need further sensitivity studies to justify the statement of "relatively minor influence of aerosol phase matrices on the inversion".

Thank you for the comment. We have added additional sensitivity experiments in Sect. 3.1 to quantify the impact of the aerosol phase matrix on the simulated TOA I and DOLP. Specifically, we conducted forward simulations using several aerosol models listed in Table 4 (which represent different phase matrices). The results indicate that the changes in both I and DOLP caused by different phase matrices are much smaller than those caused by other parameters such as AOD and SSA. This is consistent with the studies cited in L84–87.

4. L136-137: What are the exact retrieval parameters that compose the state vector? The AOD, SSA, and three RTLS parameters? At which wavelengths?

Thank you for this comment. This point is addressed in detail in our response to the General Comments #2 regarding the retrieval algorithm description. Briefly, the state vector **x** consists of aerosol and surface parameters, including AOD ($\tau(\lambda)$), SSA ($\omega(\lambda)$), kernel intensity parameters of RTLS model ($K(\lambda)$, k_{vol}, and k_{geo} in Eq. 2), and the scale factor of BPDF-NDVI model (C in Eq. 8), with wavelength-dependent parameters retrieved at 443, 490, 565, and 670 nm. The complete definition of the state vector and the corresponding wavelengths is provided in the revised manuscript and summarized in Table 3.

5. L156-158: Do you mean the x0 and Sa in Eq. (4) and Eq. (5) are derived from the statistics of multi-year datasets? If so, then:

- Which datasets (i.e., which climate models, or observations) do you use? By "multi-year", what are the exact time periods? And what are the rules for data screening?
- On a yearly and global scale, how do you take into account the variability of aerosol and surface properties and ensure no systematic bias is introduced by the a priori constraints?

- Please specify the "fixed constants" of x0 and Sa.
- And if not, please explain the way of determining the a priori constraints in more details.

Thank you for this comment. The a priori state vector $\mathbf{x}_0$ and the associated covariance matrix $\mathbf{S}_a$ in Eqs. 4 and 5 are prescribed as fixed values in this study, and are not dynamically adjusted for individual pixels or acquisition times. They are not derived from spatially or temporally varying multi-year climatological datasets.

For aerosol parameters, the a priori values and variances of AOD and SSA are derived from the mean and variance of AERONET measurements over a six-month period. The standard AERONET Level 2.0 quality-control criteria except for the AOD threshold are applied during data screening. For surface parameters, the a priori values are not derived from observational datasets. Instead, they are prescribed as fixed values summarized in Table 3, and the corresponding a priori uncertainties are defined as half of the physically plausible parameter ranges. This approach is intended to constrain the retrieval within realistic bounds without imposing observational climatology on surface properties.

The use of fixed a priori values in this study is intended to provide a controlled and consistent configuration for evaluating the algorithm's inherent retrieval capability. Under this setting, the fitting performance is not dominated by the choice of initial conditions, but is primarily determined by the information content of the multi-angle and polarimetric DPC measurements. We note that multi-year averages from climate models or other observational products could be incorporated in future applications to further improve retrieval performance, but this is beyond the scope of the present algorithm assessment.

The values of $\mathbf{x}_0$ and the diagonal elements of $\mathbf{S}_a$ used for aerosol and surface parameters have been listed in Table 3 of the revised manuscript. Further details on the retrieval configuration are provided in our response to the General Comments.

6. Section 3.1: The authors are encouraged to reduce the discussions on some already-known phenomena and focus on key features related to the retrieval accuracy, so that the section can be more refined. For example, the authors may simplify the narrative about the relationship between SSA and TOA radiance, the influence of

AOD loading on SSA sensitivity… instead, incline more to the angular and wavelength variations of the SSA sensitivity and how do they influence the selections of viewing geometry and measurement bands.

Thank you for the suggestion. We have rewritten Sect. 3.1 to make the discussion more concise and more directly linked to retrieval accuracy. In the revised text, we shortened the narrative on well-established qualitative relationships (e.g., the general dependence of TOA radiance on SSA and the effect of AOD loading on SSA sensitivity) and focused instead on the angular and spectral characteristics of SSA sensitivity. In addition, we added new sensitivity experiments and briefly compared the impacts of different parameters on I and DOLP.

7. L219: As we can see from Figure 2, ΔI for different wavelengths does not approach zero at 180° scattering angle.

We thank the reviewer for this careful observation. The reviewer is correct that ΔI does not reach zero at a scattering angle of 180°. Our original statement was intended to describe the general decreasing trend of ΔI as the scattering angle increases toward 180°, rather than implying that ΔI becomes exactly zero at that angle. We have revised the manuscript in L257 to clarify:

Overall, as the scattering angle increases, ΔI gradually decreases, indicating reduced sensitivity to SSA.

8. Figures 2-4: What is the SSA value used for producing these figures? Is the value wavelength-dependent? Why is this value chosen and considered representative?

Thank you for this important comment. The SSA used in producing Figures 2-4 is wavelength-dependent, as SSA generally varies with wavelength. To clarify its representativeness and assess its impact, we have conducted additional sensitivity experiments with SSA values ranging from 0.7 to 1.0, covering most SSA values in the actural atmosphere. The detailed experimental settings are summarized in Table 4 The analysis helps evaluate the influence of SSA assumptions on the results and support the robustness of the conclusions.

9. L226-228: Why does this sign reversal happen?

Thanks for the comment. A plausible explanation is that the wavelength dependence of the relative contributions from Rayleigh scattering, aerosol scattering, and surface reflection leads to a sign change in ΔDOLP. As wavelength increases, Rayleigh scattering (and its polarized contribution) decreases rapidly, so the TOA polarized signal becomes dominated by aerosol and surface. Around certain scattering angles, the aerosol-scattering contribution and the surface-related contribution (including atmospheric transmission of surface-reflected light) can be comparable and partially cancel. An SSA increase enhances aerosol scattering and modifies the balance between these terms. For smaller scattering angles the aerosol term tends to dominate, giving a positive ΔDOLP, whereas for larger scattering angles the surface-related term becomes relatively more important, and the same SSA perturbation can reduce DOLP, resulting in a sign reversal.

10. Figure 8 (a) and Figure 9 (a):

- What are the grids of latitude and longitude of these panels? Does the geolocation exactly match with (b) and (c)?
- The figures are not labeled with lowercase letters.

Thank you for reminding. For Fig. 8, the spatial domain of panel (a) covers 16°E–24°E and 5°S–9°S. For Fig. 9, the spatial domain of panel (a) covers 20°W–4°W and 16°N–25°N. The geolocation of panel (a) exactly matches that of panels (b) and (c) in both figures. We have added this information to the corresponding figure captions, and added lowercase letters (a), (b), and (c) to Figs. 8 and 9 in the revised manuscript.

11. L325-328: It would be interesting to compare the retrieved AOD with the corresponding MODIS product, which adds more insights on the retrieval performance when the algorithm is applied to DPC data. The same comment for the following dust event.

Thank you for this helpful suggestion. We have added VIIRS AOD maps in the Supplement. Comparisons between the retrieved AOD and the corresponding VIIRS AOD product for both the biomass burning and dust events have also been conducted. The results show that

the spatial patterns of VIIRS AOD are highly consistent with our retrievals, demonstrating good agreement in the overall distribution characteristics.

12. L334: Please refer to the last comment.

Thank you for the suggestion. As mentioned above, comparisons between the retrieved AOD and the corresponding VIIRS AOD product for the dust event have also been added in the manuscript.

13. L340-341: Looking at Figure 9, there is an obvious contrast in retrieved SSA between the region (21-23°N, 16-17°W) and the region (19-20°N, 17-19°W), while from the true color picture, the aerosols in these regions seem to be in the same type (mineral dust). What's the reason for such a contrast in SSA? Is it an artifact of the algorithm?

Thank you for this insightful comment. The apparent contrast in retrieved SSA between the two regions is likely related to differences in cross-track viewing geometry rather than changes in aerosol type. The two regions are located in different cross-track scan positions, which may introduce discontinuities in viewing geometry and associated retrieval sensitivities. Consistently, the retrieved AOD over the region (19–20°N, 17–19°W) is also relatively lower, suggesting that the SSA contrast is coupled with changes in aerosol loading and retrieval constraints.

14. L352-355: The global patterns retrieved here may not be quite comparable with the MODIS, OMI and POLDER products from the cited studies due to the differences in measurement period and wavelength. The comparison with the study of Dong et al. (TGRS, 2024) seems to bring more insights since the retrievals are from the same DPC measurements. Why don't the authors present the retrievals at 670 nm, just the same wavelength showed by Dong et al. (2024), for a more straightforward comparison?

Thank you for this insightful comment. We have added the global retrieval results at 565 nm and 670 nm in the Supplement, and compared our results with MODIS and Dong et al. (2024) in the manuscript. Overall, the patterns of AOD, SSA, and DHR retrieved in this

study are consistent with those reported by Dong et al. (2024), demonstrating similar global distribution characteristics. At the same time, some differences are observed. For example, Dong et al. (2024) reported anomalously high AOD values over South America in October 2019, whereas both our results and the MODIS AOD show relatively low values in that region. These comparisons and discussions have been incorporated into the revised manuscript to provide a more rigorous evaluation.

15. L325: "… composed of…" → be composed of

Thanks for reminding. We have revised the expression in the manuscript.

Reference

Chen, C., Dubovik, O., Fuertes, D., Litvinov, P., Lapyonok, T., Lopatin, A., et al. (2020). Validation of GRASP algorithm product from POLDER/PARASOL data and assessment of multi-angular polarimetry potential for aerosol monitoring. *Earth System Science Data*, *12*(4), 3573–3620. https://doi.org/10.5194/essd-12-3573-2020

Dong, Y., Li, J., Zhang, Z., Zheng, Y., Zhang, C., & Li, Z. (2024). Machine learning-based retrieval of aerosol and surface properties over land from the gaofen-5 directional polarimetric camera measurements. *IEEE Transactions on Geoscience and Remote Sensing*, *62*, 1–15. https://doi.org/10.1109/tgrs.2024.3419169

Dubovik, O., Herman, M., Holdak, A., Lapyonok, T., Tanré, D., Deuzé, J. L., et al. (2011). Statistically optimized inversion algorithm for enhanced retrieval of aerosol properties from spectral multi-angle polarimetric satellite observations. *Atmospheric Measurement Techniques*, *4*(5), 975–1018. https://doi.org/10.5194/amt-4-975-2011

Fang, L., Hasekamp, O., Fu, G., Gong, W., Wang, S., Wang, W., et al. (2022). Retrieval of aerosol optical properties over land using an optimized retrieval algorithm based on the directional polarimetric camera. *Remote Sensing*, *14*(18), 4571.

Hasekamp, O. P., Litvinov, P., & Butz, A. (2011). Aerosol properties over the ocean from PARASOL multiangle photopolarimetric measurements. *Journal of Geophysical Research: Atmospheres*, *116*(D14). Journal Article.

Hasekamp, O. P., Litvinov, P., Fu, G., Chen, C., & Dubovik, O. (2024). Algorithm evaluation for polarimetric remote sensing of atmospheric aerosols. *Atmospheric Measurement Techniques*, *17*(5), 1497–1525. https://doi.org/10.5194/amt-17-1497-2024

Jin, S., Ma, Y., Wang, Z., Hong, J., Chen, F., Ti, R., et al. (2024). Retrievals and performance assessment of global marine aerosol optical properties from DPC/GRASP. *Journal of Atmospheric and Environmental Optics*, *19*(6), 680–697.

Li, Z., Hou, W., Hong, J., Zheng, F., Luo, D., Wang, J., et al. (2018). Directional polarimetric camera (DPC): Monitoring aerosol spectral optical properties over land from satellite observation. *Journal of Quantitative Spectroscopy and Radiative Transfer*, *218*, 21–37. https://doi.org/10.1016/j.jqsrt.2018.07.003

Qie, L., Li, Z., Zhu, S., Xu, H., Xie, Y., Qiao, R., et al. (2021). In-flight radiometric and polarimetric calibration of the directional polarimetric camera onboard the GaoFen-5 satellite over the ocean. *Applied Optics*, *60*(24), 7186. https://doi.org/10.1364/ao.422980

Spurr, R. J. D. (2006). VLIDORT: A linearized pseudo-spherical vector discrete ordinate radiative transfer code for forward model and retrieval studies in multilayer multiple scattering media. *Journal of Quantitative Spectroscopy and Radiative Transfer*, *102*(2), 316–342. https://doi.org/10.1016/j.jqsrt.2006.05.005

Zhu, S., Li, Z., Qie, L., Xu, H., Ge, B., Xie, Y., et al. (2022). In-flight relative radiometric calibration of a wide field of view directional polarimetric camera based on the rayleigh scattering over ocean. *Remote Sensing*, *14*(5), 1211. https://doi.org/10.3390/rs14051211